Vibriobactin Antibodies: A Vaccine Strategy

Raymond J. Bergeron,*,† Neelam Bharti,† Shailendra Singh,† James S. McManis,† Jan Wiegand,† and Linda G. Green‡

Department of Medicinal Chemistry and the Hybridoma Core Laboratory, Interdisciplinary Center for Biotechnology Research, University of Florida, Gainesville, Florida 32610-0485

Received January 30, 2009

A new target strategy in the development of bacterial vaccines, the induction of antibodies to microbial outer membrane ferrisiderophore complexes, is explored. A vibriobactin (VIB) analogue, with a thiol tether, 1-(2,3-dihydroxybenzoyl)-5,9-bis[[(4*S*,5*R*)-2-(2,3-dihydroxyphenyl)-4,5-dihydro-5-methyl-4-oxazolyl]carbonyl]-14-(3-mercaptopropanoyl)-1,5,9,14-tetraazatetradecane, was synthesized and linked to ovalbumin (OVA) and bovine serum albumin (BSA). The antigenicity of the VIB microbial iron chelator conjugates and their iron complexes was evaluated. When mice were immunized with the resulting OVA−VIB conjugate, a selective and unequivocal antigenic response to the VIB hapten was observed; IgG monoclonal antibodies specific to the vibriobactin fragment of the BSA and OVA conjugates were isolated. The results are consistent with the idea that the isolated adducts of siderophores covalently linked to their bacterial outer membrane receptors represent a credible target for vaccine development.

Introduction

Iron occurs in oxidation states from −2 to +6 depending on both pH and the nature of the ligating groups surrounding the metal.[1] It is these dependencies that nature has exploited so effectively in enlisting the metal as a central component in a myriad of redox processes.[2] In fact, life without iron is virtually nonexistent.[3] However, while the metal composes some 5% of the earth's crust, it is nevertheless difficult for living systems to access. In the biosphere, iron exists largely as Fe(III), in a variety of water insoluble forms, at pH 7. The concentration of free Fe(III) under these conditions is $\sim 1.4 \times 10^{-9}$ M,[4] somewhat lower than that required to support most life forms. In the presence of phosphate ions in culture media and potential animal hosts, the free Fe(III) concentration in solution drops even further, by a factor of 10.

Both prokaryotes and eukaryotes have overcome the problem of iron accessibility by developing iron-binding ligands and associated transport systems.[5−12] Prokaryotes produce a group of iron chelators, siderophores (generally low molecular weight, iron-specific ligands), that they secrete into the environment.[10] These ligands often present very large formation constants (e.g., 10^{48} M^{-1})[13] and can effectively remove the metal from other donor arrays. The resulting metal complex, a ferrisiderophore, is then taken up by microorganisms,[14−16] most often beginning with binding to an outer membrane receptor.[17] This is followed by shuttling the iron complex through the periplasm and finally to the cytoplasm, where the iron is freed up. These ferrisiderophore transporters are energy-dependent, often exploiting the *tonB* system.[18−20] In most instances, the desferrisiderophore is released to further gather iron.

There have now been over 500 different siderophores identified.[21−25] While there are certainly exceptions, the two main classes of natural product iron chelators are hydroxamates,[26−31] such as desferrioxamine (**1**) and catecholamides,[13,32−36] including vulnibactin (**2**) and vibriobactin (**3**) (Figure 1). Some microorganisms can, in fact, utilize more than one type and/or class of siderophores.[37]

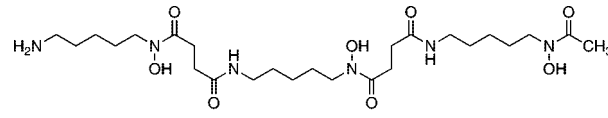

1 desferrioxamine B (DFO)

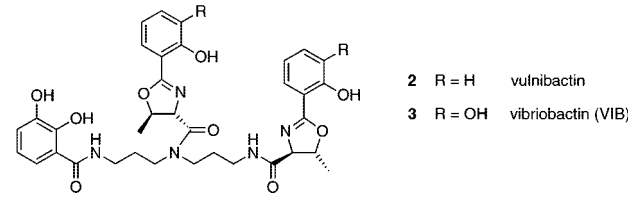

Figure 1. Naturally occurring iron chelators (siderophores): hydroxamates (**1**) and catecholamides (**2** and **3**).

Iron acquisition becomes somewhat more problematic for microorganisms in an in vivo situation (e.g., in humans). Pathogens have additional iron acquisition hurdles to overcome beyond low metal solubility. Animals, for example, have an iron-withholding system: proteinaceous iron chelators that make iron acquisition difficult for microorganisms. There is little of the free metal available in animals. It is generally bound to heme[10] (iron-containing enzymes)[10] by transferrin[12] (an iron shuttle protein) or stored in ferritin.[11] In each instance, iron is not easily accessible to microorganisms.

The opportunistic microorganism *Vibrio vulnificus* nicely illustrates how pathogens can overcome host iron-withholding.[20,38] The siderophore produced by *Vibrio vulnificus*,[21] vulnibactin (**2**) (Figure 1), cannot remove iron from transferrin, the ever-present iron shuttle protein in plasma, in spite of the fact that **2** binds iron more tightly than transferrin. The chelator cannot access transferrin iron, as it is bound within the protein. To solve this problem, the microorganism secretes a protease, which cleaves transferrin, thus releasing iron. The metal is then sequestered by **2**, and the ferrisiderophore is taken up via an intermembrane receptor *viuA*.[39−41]

In fact, *Vibrio vulnificus* mutants without the vulnibactin transporter have reduced pathogenicity in mice.[42] This uptake apparatus has been shown to have significant homology with the *Vibrio cholerae* receptor.[20,38,39] However, while it seems

* To whom correspondence should be addressed. Phone: (352) 273-7725. Fax: (352) 392-8406. E-mail: rayb@ufl.edu.
† Department of Medicinal Chemistry.
‡ Hybridoma Core Laboratory, Interdisciplinary Center for Biotechnology Research.

10.1021/jm900119q CCC: $40.75
Published on Web 06/03/2009

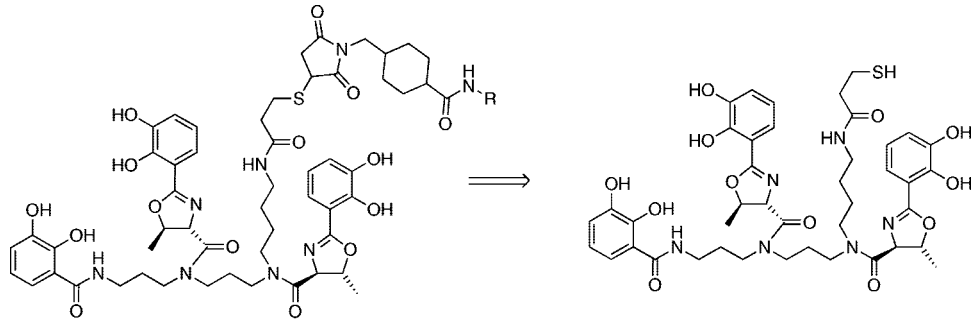

4 R = OVA (OVA-VIB)

5 R = BSA (BSA-VIB)

6

Figure 2. Retrosynthetic analysis of vibriobactin-OVA (**4**) and vibriobactin−BSA (**5**) conjugates from vibriobactin thiol (**6**).

clear from studies with genetically altered microorganisms that shutting down the siderophore iron-uptake system can slow growth and reduce pathogenicity, microorganisms can still access iron via other mechanisms.[43−45] For example, *Vibrio cholerae* can utilize transferrin and heme as iron sources. The issue then becomes how useful a target the siderophore transport apparatus is in antimicrobial design strategies.

Miller has, in a series of classic studies, employed siderophores and the corresponding transporters as vectors for the delivery of antibiotics.[46] Alternatively, Esteve-Gassent was able to demonstrate that a vaccine developed to treat eels infected with *Vibrio vulnificus* serovar E. contained antigens to the putative receptor for vulnibactin. Esteve-Gassent point out that the antibody could be blocking siderophore uptake, could trigger classical complement activation, or "mark bacteria for opsonophagocytosis".[47]

There is now significant literature that supports the idea that many microorganisms present with outer membrane receptors for the binding and internalization of their ferrisiderophore complexes. It is not unreasonable to assume that on binding to the microbial receptors, the iron siderophore complex is at least initially exposed. If sufficiently antigenic, this "ferrisiderophore face" could represent a significant target in vaccine development. The question then becomes what should the expectations be regarding the antigenicity of a ferrisiderophore fixed to a large carrier molecule? If indeed it were very antigenic, this would merit the assembly of ferrisiderophores with functionality that allow for covalent linkage to the transporter and isolation of the adduct as a potential vaccine.

The antigenicity of a ferrisiderophore bound to a large carrier molecule is the focus of this manuscript. The specific questions addressed here are the following: Is it possible (1) to assemble a carrier siderophore conjugate, i.e., a protein carrier conjugate, (2) to raise antibodies to the conjugate in mice, and (3) to assess the antigenicity of the protein siderophore and its iron complex?

Results and Discussion

Antigen Design Concept. The current study focuses on the generation of antibodies against vibriobactin (**3**, VIB[a]), the hexacoordinate iron chelator, a siderophore, responsible for iron utilization in *Vibrio cholerae*.[48,49] This was attractive for two reasons: *Vibrio cholerae* represents an important pathological target,[50−52] and we had established critical information about vibriobactin chemistry in earlier studies.[32−36] Accordingly, we elected to investigate an ovalbumin (OVA)−vibriobactin protein conjugate (**4,** OVA−VIB) as an antigen.

The fundamental issue would be appending a tether to vibriobactin (**3**) (Figure 1), which would allow for fixing the ligand to a carrier protein, in this case, both OVA and bovine serum albumin (BSA). This demanded a synthetic approach very different from the assembly of vibriobactin itself.[35] The OVA−VIB conjugate (**4**) would be used as an antigen to raise antibodies in mice, and the BSA−VIB conjugate (**5**) (Figure 2) would be utilized in an enzyme-linked immunosorbent assay (ELISA), first for the detection of serum polyclonal antibodies and, finally, vibriobactin-specific IgG monoclonal antibodies. Thus, choosing the appropriate activated tether for the vibriobactin protein conjugate was the first hurdle. While a number of different tethers were considered (e.g., acyl, halo, thiol), previous experience with hypusine antibody generation[53] encouraged pursuit of a thiol-containing tether. The final ligand would be 1-(2,3-dihydroxybenzoyl)-5,9-bis[[(4*S*,5*R*)-2-(2,3-dihydroxyphenyl)-4,5-dihydro-5-methyl-4-oxazolyl]carbonyl]-14-(3-mercaptopropanoyl)-1,5,9,14-tetraazatetradecane (**6**) or vibriobactin thiol (Figure 2).

The first approach to vibriobactin thiol (**6**) began with the conversion of norspermidine (**7**) to polyamine reagent **12**, that is, thermospermine[54] protected at the aminobutyl terminus (Scheme 1). Specifically, norspermidine (**7**) was heated at reflux with 4-chloro-1-butanol in 1-butanol in the presence of K_2CO_3 and KI, producing linear triamino alcohol **8**. The amine groups of **8** were masked as *tert*-butyl carbamates using di-*tert*-butyl dicarbonate in THF to generate alcohol **9** in 42% yield for two steps. In spite of the moderate yield, the conversion of **7** to **9** in Scheme 1 is considerably shorter than our previous route to N^1-(4-hydroxybutyl)-N^1,N^4,N^7-tris(*tert*-butoxycarbonyl)norspermidine (**9**).[55] The hydroxyl of **9** was activated as its tosylate **10** in 92% yield by treatment with TsCl in CH_2Cl_2 and NEt_3.[55] Heating **10** with potassium phthalimide in DMF at 85 °C gave the fully protected tetraamine **11** in 71% yield. The carbamates of **11** were cleaved quantitatively with trifluoroacetic acid (TFA), affording reagent **12**. Activation of 2,3-dimethoxybenzoic acid with 1,1′-carbonyldiimidazole (CDI) and acylation of the primary amine of **12** in CH_2Cl_2 and NEt_3 gave masked catecholamide **13** in 70% yield. Next, the *N*-hydroxysuccinimide ester of *N*-*tert*-butoxycarbonyl-L-threonine[56] (3 equiv) was coupled to the internal nitrogens of **13** in DMF to produce

[a] Abbreviations: VIB, vibriobactin; BSA, bovine serum albumin; OVA, ovalbumin; ELISA, enzyme-linked immunosorbent assay; TFA, trifluoroacetic acid; CDI, 1,1′-carbonyldiimidazole; OD, optical density; ICP-MS, inductively coupled plasma mass spectroscopy; NMS, normal mouse sera; sc, subcutaneously; EWB, ELISA wash buffer; PBS, phosphate buffered saline; mAb, monoclonal antibody; DMSO, dimethyl sulfoxide; THF, tetrahydrofuran; DMF, *N*,*N*-dimethylformamide.

Scheme 1. Synthesis of **17**[a]

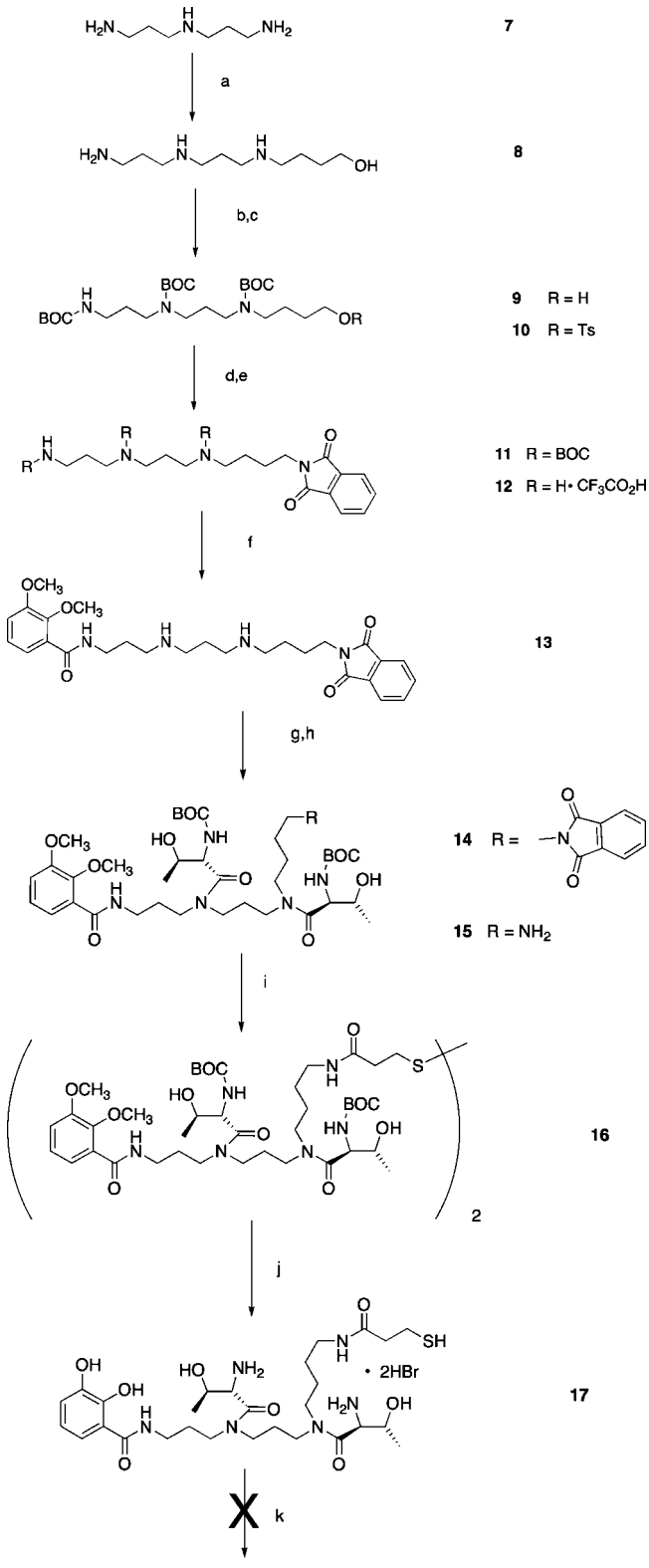

[a] Reagents: (a) 4-chloro-1-butanol, K_2CO_3, KI, 1-butanol, 125 °C, 1 d; (b) di-*tert*-butyl dicarbonate, THF, 42%; (c) 92%;[55] (d) potassium phthalimide, DMF, 90 °C, 48 h, 71%; (e) TFA, CH_2Cl_2, 0 °C → room temp, 2 h, quantitative; (f) 2,3- dimethoxybenzoic acid, CDI, CH_2Cl_2, NEt_3, 70%; (g) *N*-(BOC)-L-threonine *N*-hydroxysuccinimide ester (3 equiv), DMF, 55%; (h) hydrazine hydrate, EtOH, 65%; (i) 3,3′-dithiopropionic acid (0.4 equiv), CDI, CH_2Cl_2, 40%; (j) BBr_3, CH_2Cl_2, 73%; (k) ethyl 2,3-dihydroxybenzimidate, failed.

triamide **14** in 55% yield. The phthalimide protecting group of **14** was removed in 65% yield with hydrazine hydrate in EtOH, generating primary amine **15**, 2 equiv of which were connected using 3,3′-dithiodipropionic acid (CDI in CH_2Cl_2), furnishing disulfide **16** in 40% yield. Threonylamine and catecholamide deprotection and also disulfide cleavage occurred in the presence of BBr_3 in CH_2Cl_2, giving dihydrobromide salt **17** in 73% yield. Unfortunately, any attempt at cyclization of the threonyl fragments of **17** with ethyl 2,3-dihydroxybenzimidate[34] resulted in complex mixtures, including thioesters, that were virtually impossible to separate, thus dooming the route of Scheme 1 to failure in the last step.

Scheme 2. Synthesis of **20**[a]

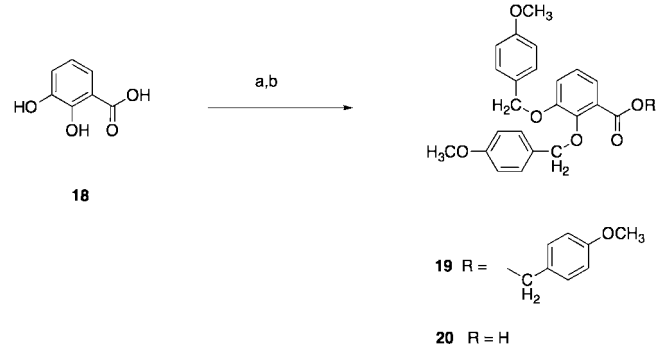

[a] Reagents: (a) 60% NaH, 4-methoxybenzyl bromide (3.5 equiv), DMF, 62%; (b) 2 N NaOH, dioxane, 90%.

A catechol protecting group other than methyl, that is, one that could be removed concurrently with the BOC functionality while leaving the disulfide intact, was required. Thus, 2,3-dihydroxybenzoic acid (**18**) was converted to its trianion with NaH in DMF and treated with excess 4-methoxybenzyl bromide to make ester **19** in 62% yield. Hydrolysis of **19** with NaOH (aqueous) in dioxane produced 2,3-bis(4-methoxybenzyloxy)-benzoic acid (**20**) in 90% recrystallized yield (Scheme 2). Activation of an equivalent of carboxylic acid **20** with CDI and stirring with N^{12}-(phthaloyl)thermospermine (**12**) in CH_2Cl_2 and NEt_3 afforded diamine **21** in 57% yield (Scheme 3).

The secondary amines of **21** were acylated with the active ester of *N*-(BOC)-L-threonine as before to generate tetraamine derivative **22** in 60% yield. The phthalimide functionality of **22** was cleaved in 90% yield with hydrazine hydrate in EtOH at room temperature, yielding primary amine **23**, 2 equiv of which were joined utilizing 3,3′-dithiodipropionic acid (CDI in CH_2Cl_2), resulting in disulfide **24** in 60% yield. The threonyl carbamates and the 4-methoxybenzyl ethers[57] of **24** were simultaneously cleaved, using TFA in anisole and CH_2Cl_2; Sephadex LH-20 purification resulted in a 60% yield of disulfide **25**, a tetrakis(TFA) salt. The threonyl moieties of **25** were next condensed with excess ethyl 2,3-dihydroxybenzimidate[34] in refluxing EtOH to produce tetrakis(oxazoline) disulfide **26** in 20% yield. Finally, the disulfide bond of iron chelator **26** was reduced to the free thiol **6** in 60% yield, utilizing H_2 (3 atm) over Pd black in CH_3OH under iron-free conditions (Scheme 3).

Functionalization of Vibriobactin Thiol (6) with OVA and BSA Protein Carriers. Vibriobactin thiol (**6**), freshly generated from disulfide **26** (Scheme 3), was incubated with a maleimide-activated OVA (**27**) or BSA (**28**) protein carrier for 8 h. Unreacted maleimide was capped by conjugating it further with cysteine for 8 h, resulting in Michael adduct OVA−VIB (**4**) or BSA−VIB (**5**), respectively (Scheme 4). Both **4** and **5** were purified on a dextran desalting column. Positive fractions, as determined by the optical density (OD) at 280 nm, were analyzed for protein concentration using a Coomassie assay.[58]

Scheme 3. Synthesis of Vibriobactin Thiol **6**[a]

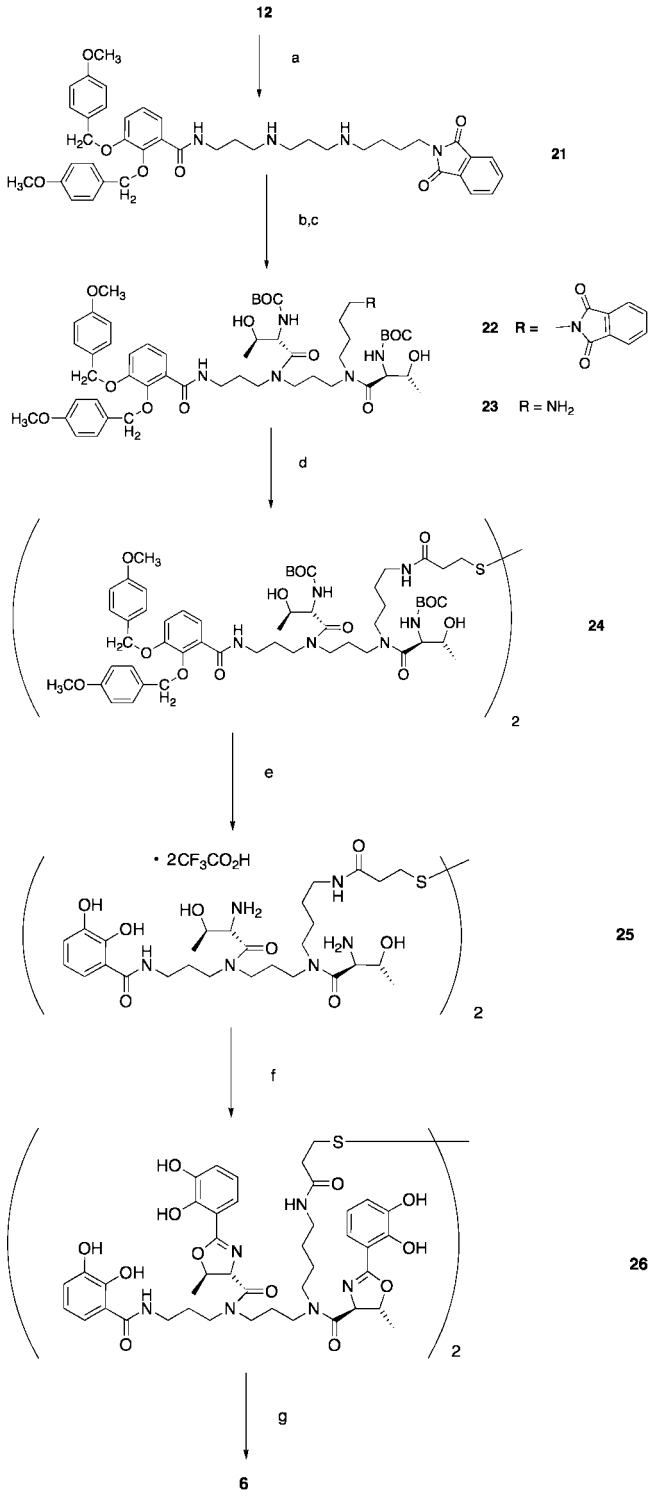

[a] Reagents: (a) **20**, CDI, CH_2Cl_2, NEt_3, 57%; (b) *N*-(BOC)-L-threonine *N*-hydroxysuccinimide ester (2.5 equiv), DMF, 40 °C, 60%; (c) hydrazine hydrate, EtOH, 90%; (d) 3,3′-dithiopropionic acid, CDI, CH_2Cl_2, NEt_3, 60%; (e) TFA, anisole, CH_2Cl_2, 0 °C → room temp, 2 h, 60%; (f) ethyl 2,3-dihydroxybenzimidate, EtOH, reflux, 36 h, 20%; (g) H_2, 3 atm, Pd black, EtOH, 1 d, 60%.

Functionalities **29** and **30** were also generated (Scheme 4); **30** was used as a negative control in evaluating the capacity of **6** as an antigenic determinant when bound to BSA.

Iron Complexes of 4, 27, 3, and 26. Protein desferrivibriobactin−OVA complex **4** was converted to the corresponding ferric siderophore complex **31** by mixing the conjugate with

Scheme 4. Coupling of Vibriobactin Thiol **6** to Carrier Proteins[a]

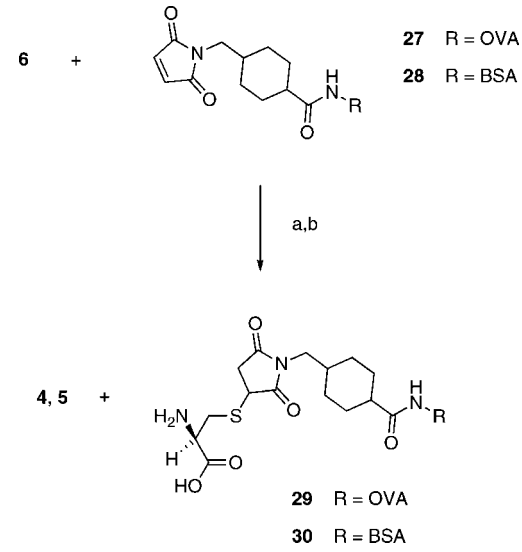

[a] Reagents: (a) 50% DMSO, 0.1 M phosphate buffer (pH 7.4), 8 h; (b) cysteine.

excess ferric nitrilotriacetate in phosphate buffer for 2 h. At this point, desferrioxamine (**1**) (Figure 1) was added to complex excess iron. The mixture was then purified on a G-25 Sepharose column. The same ferration procedure, including purification, was carried out on the maleimide-activated OVA (**27**), producing ferric protein complex **32**. The iron content of the purified ferrivibriobactin protein adduct (**31**), the iron-treated maleimide protein (**32**), and the elution buffer were determined by inductively coupled plasma mass spectroscopy (ICP-MS). The background iron, elution buffer iron, and maleimide protein iron were subtracted from the iron content associated with the ferrivibriobactin OVA complex (**31**). From this measurement, and assuming that Fe(III) and vibriobactin form a 1:1 complex, the coupling efficiency of OVA maleimide (**27**) to **6** was 30%.

Vibriobactin (**3**) and vibriobactin disulfide (**26**) iron(III) complexes, **33** and **34**, respectively, which were to be evaluated as potential antigens, were prepared as previously described.[59] The resulting suspensions were separated on a small C-18 column, eluting with EtOH (aqueous). Colored fractions were pooled and lyophilized.

Development of Murine Monoclonal Antibodies against Vibriobactin. The procedures were similar to those of Kao and Klein[60] and Simrell, et al.[61] Briefly, the OVA−VIB conjugate (**4**) was used as an antigen to raise antibodies in mice. Antigenic response was determined via an ELISA. Once an adequate IgG response was observed, an immunized mouse was given a final, prefusion booster of the antigen without adjuvant. The mouse was euthanized 4 days later, and antibody-forming cells from the animal's spleen were fused to tumor cells grown in culture. The resulting hybridomas were screened for antibody production; antibody-producing hybridomas were cloned. Monoclonal antibodies were then produced and purified.

Polyclonal Antibody Response. Two mice (M1 and M2) were immunized with **4**. The immune response (serum titer) of these animals and nonimmunized mice (normal mouse sera, NMS) was determined via ELISA for polyclonal antibodies against the following potential antigens: (a) BSA−VIB conjugate (**5**), (b) BSA−cysteine conjugate (**30**), (c) vibriobactin thiol (**6**), (d) vibriobactin disulfide (**26**), (e) vibriobactin disulfide−iron complex (**34**), (f) vibriobactin (**3**), and (g) vibriobactin−iron complex (**33**). Twenty-three days after the second immunization,

Table 1. ELISA Determination of Reactivity of Polyclonal Antibodies (Serum Titer) against **5** and **30**

	optical density at 405 nm[a]								
	M1			M2			NMS		
serum dilution	**5**		**30**	**5**		**30**	**5**		**30**
	23 d	56 d	56 d	23 d	56 d	56 d	23 d	56 d	56 d
1:200	3.192	3.675	3.464	3.381	3.647	3.496	0.111	0.111	0.087
1:400	3.295	3.749	3.340	3.370	3.692	3.496	0.106	0.095	0.077
1:800	2.986	3.708	2.787	3.148	3.664	3.359	0.113	0.107	0.074
1:1600	2.230	3.586	1.676	2.867	3.637	2.975	0.087	0.087	0.072
1:3200	1.370	3.535	0.883	2.188	3.486	2.025	0.109	0.096	0.076
1:6400	0.905	2.919	0.447	1.255	2.724	1.270	0.179	0.100	0.072
1:12800	0.476	1.756	0.254	0.809	1.718	0.736	0.106	0.095	0.080
1:25600	0.296	0.830	0.167	0.431	1.012	0.379	0.100	0.091	0.094

[a] The optical density of the *p*-nitrophenol product was determined 1 h after the addition of the *p*-nitrophenyl phosphate substrate. M1 was immunized with **4** twice sc at a dose of 50 μg/immunization. M2 was immunized with the conjugate twice sc at 100 μg/immunization. Sera were obtained 23 and 56 d after the second immunization. Normal mouse sera (NMS) served as a negative control.

the serum from the mouse immunized with a higher dose of **4** (M2) seemed more active against antigen **5** than M1, with a higher *p*-nitrophenol OD at 405 nm at all dilutions (Table 1). However, by day 56, there was little difference in the reactivity of serum from M1 vs M2. At this time, even after a 25600-fold dilution, the serum titers of the immunized mice against **5** were over 9 times greater than that of the NMS (Table 1).

The mouse sera also contained polyclonal antibodies against **30** that were nearly as active as antibodies against **5** (Table 1). Since cysteine was used to cap unreacted maleimide sites in the synthesis of **4**, this was expected. As will be discussed below, this was not an issue for the purified monoclonal antibodies; we were able to select for antibodies specific against **4**. The mouse sera did not react against any of the other antigens, c−g (data not shown). This could have been attributed to a simple lack of activity in the case of antigens c−g or the nature of the ELISA itself. Antigens c−g are relatively low molecular weight, moderately water-soluble ligands. These compounds may not have adhered to the ELISA wells, or they may have been removed during the washing steps. In order to settle this issue, a series of competitive binding ELISAs were performed.

Competitive Binding ELISA. In the competitive binding ELISA, sera from immunized mice or nonimmunized mice were first incubated with potential antigens f and g, or with **4**, at antigen concentrations ranging from 0 to 250 μg/mL. If an antigen is an effective competitor, it will bind to the antibody during this initial incubation, leaving less antibody available to bind to a second antigen coated on the ELISA plate. This "competition" will be reflected in lower *p*-nitrophenol optical density values.

Antigen **4** was found to be an effective competitor at all concentrations tested (Figure 3, Table 2). The smaller antigens f and g were not effective competitors (data not shown), verifying the necessity for a large carrier molecule in order for the antibody to recognize vibriobactin (**3**). Unconjugated OVA (**27**) was not an effective competitor. The *p*-nitrophenol optical density of serum incubated with **27** against antigen **5** was 92% greater than serum first incubated with **4** at the same concentration (Figure 3). It is clear that the antibody "recognizes" the siderophore on the protein carrier.

Cell Fusion−Hybridoma Formation. Four months after the second immunization, mouse M2 was given a prefusion booster of **4**. Fusion was done following the method of Simrell et al.[61] except that the myeloma cell line used was Sp2/0. In short, spleen cells were fused with Sp2/0 cells such that the ratio of

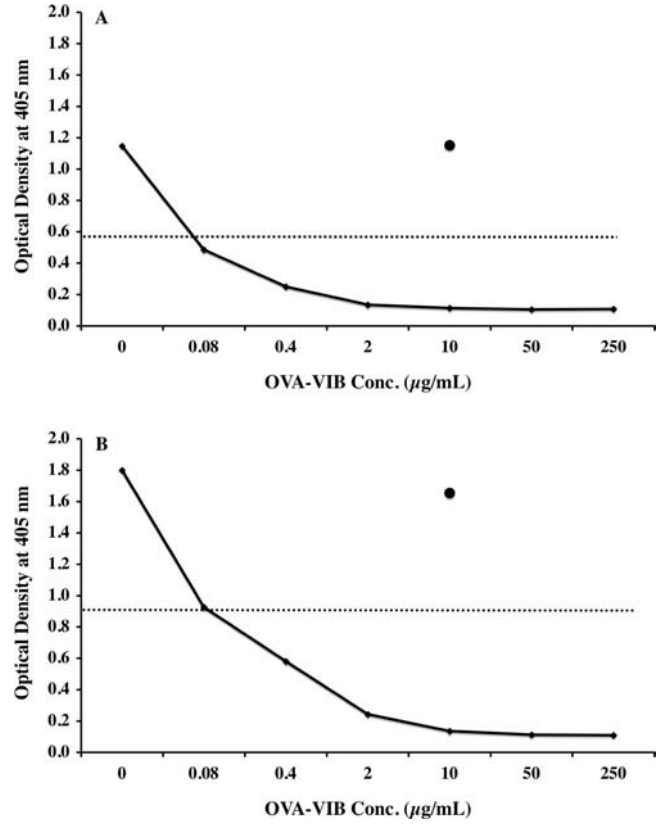

Figure 3. Competitive binding ELISA of diluted polyclonal sera (1:10000) from mice immunized with the OVA−VIB conjugate (**4**). Animal M1 (**A**) was immunized with **4** twice sc at 50 μg/injection, while mouse M2 (**B**) was immunized with **4** twice sc at 100 μg/injection. The sera were incubated with varying concentrations of antigen **4**, prior to being tested via ELISA against antigen **5**. The dotted line indicates the amount of **4** (~0.05 μg/mL) needed to reduce the optical density of the *p*-nitrophenol product to 50% of that of the sera not incubated with any **4**. The closed circles indicate the optical density of unconjugated OVA (**27**) (10 μg/mL).

Table 2. Competitive Binding ELISA of Serum from Immunized Mice and Nonimmunized Mice

antigen **4** conc (μg/mL)	antigen **5**: optical density at 405 nm[a]		
	M1	M2	NMS
0	1.147	1.800	0.113
0.08	0.486	0.926	0.109
0.4	0.250	0.581	0.108
2	0.135	0.243	0.105
10	0.114	0.137	0.108
50	0.106	0.113	0.108
250	0.108	0.109	0.111
Medium	0.048	0.044	0.045
27	1.152	1.655	0.113

[a] The optical density of the *p*-nitrophenol product was determined 1 h after the addition of the *p*-nitrophenyl phosphate substrate. Sera from immunized mice (M1 and M2) and normal mice (NMS), diluted 1:10000, were incubated with antigen **4** for 2 h at room temperature. A portion of this mixture was then transferred to an ELISA plate that had been coated with antigen **5**, 10 μg/mL. Medium was used as a negative control; unconjugated OVA (**27**) (10 μg/mL) served as a positive control.

spleen cells to Sp2/0 cells was 7:1. After incubation for 11 days, the supernatants from the resulting hybridomas were tested via ELISA against antigen **5**. The hybridomas that gave the strongest ELISA signal were further cultured for 7 days. Their supernatants were tested again via ELISA against **5**, BSA−VIB−iron (**35**), and **30**. The class of antibody (IgG or IgM) was also determined. The 12 most active hybridomas that were **5** and **35** positive and **30** negative are shown in Table 3. One hybridoma,

Table 3. Reactivity of Antibody-Containing Hybridoma Supernatants against **5** and Other Antigens as Measured by an ELISA

	optical density at 405 nm[a]				
hybridoma	**5**	**35**	**30**	IgG (γ-chain)	IgM (μ-chain)
1H8	3.662	3.040	0.100	0.608	0.091
2C11	3.564	3.427	0.246	3.652	0.432
2D6	2.481	2.340	0.157	0.825	3.083
2F5	3.173	2.832	0.180	3.530	0.120
2F10	2.830	2.903	0.161	2.331	0.085
3F11	3.331	3.449	0.217	3.537	0.133
3H9	2.824	3.663	0.486	3.808	0.389
4A5	1.979	2.022	0.196	2.491	0.084
4A7	3.154	2.962	0.555	3.532	0.094
4G3	2.399	2.130	0.170	3.500	0.097
5A6	3.359	3.488	0.390	2.889	0.090
5D8	4.000	4.000	0.548	4.000	0.120
Medium	0.093	0.101	0.107	0.103	0.106
M2 (PC)	3.350	3.443	1.002	3.438	0.386

[a] The optical density of the *p*-nitrophenol product was determined 1 h after the addition of the *p*-nitrophenyl phosphate substrate. Medium served as a negative control; immune mouse serum (M2) in a 1:1000 dilution was used as a positive control (PC). Hybridoma culture supernatants were undiluted and were screened for antigenic activity 18 days postfusion. Rabbit antimouse IgG (whole molecule), at a dilution of 1:1000, was used to assess the reactivity of the BSA-containing antigens. The class of antibody (IgG or IgM) was determined by the use of goat antimouse IgG (γ-chain specific) or goat antimouse IgM (μ-chain specific) at a dilution of 1:4000.

2D6, was IgM-positive; the remaining 11 hybridomas were IgG-positive (Table 3). Two of the most promising IgG-positive hybridomas, 5A6 and 2F10, were cloned.

Cloning of Antibody-Producing Hybridomas. Cells from the 5A6 and 2F10 hybridomas were diluted to a concentration of one or two cells per well. After incubation for 4 days, the plates were scanned microscopically and were scored for single colony and multiple colony wells. Ten days after seeding, supernatant from the wells that contained cells underwent screening via ELISA against **5**. Supernatants from the single colony wells of 5A6 were not very active against **5** (data not shown). Because of this, the four most **5** positive multiple colony wells of 5A6 were pooled, diluted, and replated as single cells. After 10 days, supernatants from the resulting clones were tested by an ELISA against **5**. The 10 single colony wells with the strongest ELISA positives (primary) against **5** are shown in Table 4. After incubation for an additional 5 days, the supernatants were tested again (secondary) via ELISA against **5**, **35**, and **30**. All 10 clones were highly active against **5** and **35** and showed little activity toward **30** (Table 4). A positive **5** and **35** response and a negligible **30** response were a clear indication that the antigenic determinants of the antibody were associated with the vibriobactin (**3**) segment of **5** and not with BSA (**28**) itself.

Recloning of the 2F10 hybridoma was unnecessary: 2F10−1A9 and 2F10−2A3 were highly active against **5** and **35** and poorly responsive to **30** (Table 5). These two clones, as well as two clones from 5A6 (5A6−2D5 and 5A6−1G8), were selected for further evaluation. The clone supernatants were assayed for the class of antibody, IgG or IgM, and were shown to be IgG-positive (Table 5). Multiple stocks from each cell line were frozen. 5A6−1G8 and 2F10−2A3 were tested for mycoplasma contamination and were found to be negative. Additional monoclonal antibodies (mAb) derived from 5A6−2D5 and 2F10−1A9 were produced and purified.

Competitive Binding ELISA Studies: Determination of the Sensitivity of the Purified Monoclonal Antibodies. Competitive binding ELISA studies using the purified mAb were conducted. The mAb were first incubated with varying concentrations of antigen **4**, from 0 to 250 μg/mL, prior to being transferred to an ELISA plate that had been coated with antigen **5**. Antigen **4** was found to be an effective competitor at all concentrations tested (Figure 4, Table 6); **27** was not an effective competitor. The *p*-nitrophenol optical density of the mAb initially incubated with **27** against antigen **5** was approximately 90% greater than those of the mAb first incubated with **4** at the same concentration (Table 6). It is clear that the antibody "recognizes" the siderophore on the protein carrier.

Table 4. Recloning of 5A6 Pooled Multiple Colony Wells: ELISA Screening of Supernatants from Resulting Single Colony Wells against **5**, **35**, and **30**

	optical density at 405 nm[a]			
	5			
clone	primary	secondary	**35**	**30**
1G2	4.000	3.472	3.492	0.721
1G8	4.000	3.558	3.444	0.807
2D5	3.408	3.575	3.579	0.689
2F4	3.382	3.522	3.586	0.831
2G4	3.436	3.548	3.587	1.075
3B9	3.395	3.473	3.418	1.130
3E9	3.395	3.420	3.386	0.604
3G8	3.457	3.479	3.549	0.929
4B5	3.421	3.503	3.534	0.636
4B7	3.419	3.503	3.563	0.862
Medium	0.235	0.125	0.127	0.099
5A6 (PC)	3.359	3.488	3.488	0.667

[a] The optical density of the *p*-nitrophenol product was determined 1 h after the addition of the *p*-nitrophenyl phosphate substrate. Medium was used as a negative control; supernatant from the pooled multiple colony wells from 5A6 served as a positive control (PC). Hybridoma clone culture supernatants were undiluted and were assessed for activity against **5** 10 days after recloning (primary). The hybridomas were incubated for an additional 5 days, and the supernatants were screened again (secondary). Activity against **35** and **30** were determined 15 days after recloning.

Table 5. Reactivity of 5A6 and 2F10 Clone Supernatant against **5** and Other Antigens As Measured by an ELISA

	optical density at 405 nm[a]				
clone	**5**	**35**	**30**	IgG (γ-chain)	IgM (μ-chain)
5A6−1G8	3.613	3.565	0.663	3.610	0.220
5A6−2D5	3.576	3.443	0.792	2.825	0.460
5A6 (PC)	3.359	3.488	0.667	3.659	0.250
2F10−1A9	3.410	3.335	0.413	3.522	0.413
2F10−2A3	2.675	2.656	0.300	2.825	0.460
2F10 (PC)	2.347	2.185	0.362	2.729	0.301
Medium	0.172	0.155	0.166	0.192	0.315

[a] The optical density of the *p*-nitrophenol product was determined 1 h after the addition of the *p*-nitrophenyl phosphate substrate. Hybridoma clone culture supernatants were undiluted. Medium served as a negative control; supernatant from the pooled multiple colony wells from 5A6, and supernatant from the 2F10 uncloned parent hybridoma, served as positive controls (PC). Rabbit antimouse IgG (whole molecule), at a dilution of 1:1000, was used to assess the reactivity of the BSA-containing antigens. The class of antibody (IgG or IgM) was determined by the use of goat antimouse IgG (γ-chain specific) or goat antimouse IgM (μ-chain specific) at a dilution of 1:4000.

Antigenic Determinants. One of the observations that stands out with the data from the antibody-containing hybridoma supernatants is the lack of difference in reactivity between **5** and its iron complex (**35**) (Tables 3 and 5). There are profound differences in structure between vibriobactin (**3**) and its 1:1 iron complex (**33**). Complex **33** would have all of the donor groups (e.g., aromatic hydroxyls and oxazoline nitrogen) folded into the metal.[48] Catecholamides such as **3** bind iron very tightly, with formation constants of nearly 10^{48} M^{-1}.[13] This means that because of the ubiquitous nature of iron, the iron complexes **31** and **35** were probably formed in vitro. In fact, it is likely that antibodies in animals are being formed against the OVA−VIB iron complex (**31**).

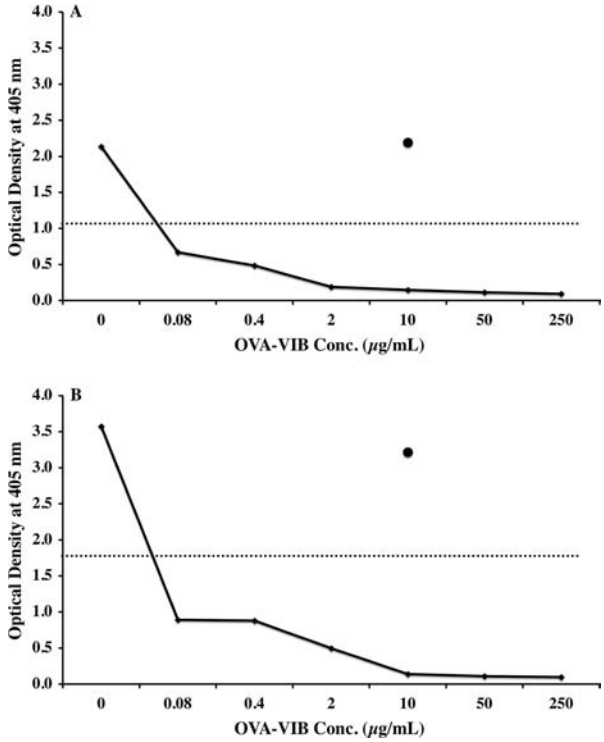

Figure 4. Competitive binding ELISA of purified mAb from 5A6−2D5 (A) and 2F10−1A9 (B). The mAb (0.11 μg of protein/mL) were incubated with varying concentrations of antigen **4**, prior to being tested via ELISA against antigen **5**. The dotted line indicates the amount of **4** (~0.05−0.06 μg/mL) needed to reduce the optical density of the *p*-nitrophenol product to 50% of that of the mAb not incubated with any **4**. The closed circles indicate the optical density of **27** (10 μg/mL).

Table 6. Competitive Binding ELISA of Purified Monoclonal Antibodies Derived from Clones of 5A6−2D5 and 2F10−1A9

	antigen **5**: optical density at 405 nm[a]	
antigen **4** conc (μg/mL)	5A6−2D5 (purified mAb)	2F10−1A9 (purified mAb)
0	2.132	3.572
0.08	0.669	0.889
0.4	0.483	0.879
2	0.189	0.497
10	0.145	0.137
50	0.113	0.109
250	0.093	0.095
medium	0.092	0.090
27	2.190	3.214

[a] The optical density of the *p*-nitrophenol product was determined 1 h after the addition of the *p*-nitrophenyl phosphate substrate. Purified monoclonal antibodies (mAb) were incubated with antigen **4** for 2 h at room temperature. A portion of this mixture was then transferred to an ELISA plate that had been coated with antigen **5**, 10 μg/mL. Medium was used as a negative control; **27** (10 μg/mL) served as a positive control.

To support this idea, bile duct-cannulated rats were given **3** subcutaneously (sc) at a dose of 75 μmol/kg. The rodents' bile and urine were collected for 48 h to determine if **3** sequestered and promoted the excretion of iron. The iron content of the bile and urine was determined using atomic absorption spectroscopy. We have used this model for many years to evaluate the efficiency with which iron chelators promote the excretion of iron from animals.[62,63] Vibriobactin (**3**) was indeed found to sequester iron in vivo. Recall that **3** forms a tight 1:1 iron complex with Fe(III). Rats given 75 μmol/kg of **3** would be expected to clear 75 μg atoms/kg of iron if the binding and clearance were 100% efficient. However, the iron clearing efficiency of **3** in the rats, i.e., the actual amount of iron cleared by the ligand vs the theoretical iron clearance, was only 4.3 ± 1.1%. This implied that up to 95% of the free ligand remains or is cleared uncomplexed. In the bile duct-cannulated rats this, of course, all unfolds in a matter of hours. However, in the mouse immunization experiments, **4** had *weeks* to become saturated with iron; the most important issue is the iron to ligand ratio. Assuming that 3.23 μg atoms of iron/kg is available for chelation, in a 25 g mouse 1.45×10^{-9} mol of iron is available. The mice were effectively given 0.33×10^{-9} (M1) or 0.66×10^{-9} (M2) mol of **4**. In view of the protracted exposure of the ligand to iron, it is difficult to imagine that all of the **3** bound to OVA would also not be iron-bound.

Conclusion

The current study focused on methodologies for assembling antigens that would allow for the assessment of the antigenic properties of vibriobactin fixed to large carrier molecules, e.g., OVA (**27**) and BSA (**28**). Choosing the appropriate activated tether for the vibriobactin protein conjugate was the first hurdle. While a number of different tethers were considered, a thiol analogue was chosen, 1-(2,3-dihydroxybenzoyl)-5,9-bis[[(4*S*,5*R*)-2-(2,3-dihydroxyphenyl)-4,5-dihydro-5-methyl-4-oxazolyl]carbonyl]-14-(3-mercaptopropanoyl)-1,5,9,14-tetraazatetradecane (**6**) or vibriobactin thiol (Figure 2).

The first attempt at synthesizing **6** (Scheme 1) unfortunately failed in the last step. Cyclocondensation of ethyl 2,3-dihydroxybenzimidate[34] with the threonyl units of thiol **17** led to intractable mixtures, including thioesters. It became clear that the free thiol could not be released prior to this cyclocondensation. In a second approach (Scheme 2), a different catechol protecting group was employed in 2,3-bis(4-methoxybenzyloxy)benzoic acid (**20**). This could be removed concurrently with the BOC functionality of the key intermediate **24** to produce **25** while leaving the requisite disulfide intact (Scheme 3). The threonyl moieties of **25** were next condensed with excess ethyl 2,3-dihydroxybenzimidate.[34] Finally, disulfide iron chelator **26** was cleaved to the vibriobactin thiol (**6**), utilizing H_2 (3 atm) over Pd black in CH_3OH under iron-free conditions (Scheme 3). The thiol (**6**) was then incubated with a maleimide-activated OVA (**27**) or BSA (**28**) protein carrier, resulting in Michael adduct OVA−VIB (**4**) or BSA−VIB (**5**), respectively (Scheme 4). Conjugate **4** was mixed with an adjuvant and was successfully used as an antigen to raise antibodies in mice, and conjugate **5** was used in an ELISA, first for the detection of serum polyclonal antibodies and ultimately vibriobactin-specific IgG monoclonal antibodies.

It is clear that further characterization of the antibody−antigen binding is required, e.g., stoichiometries, formation constants, etc. The results to date are consistent with the idea that vibriobactin (**3**) presents strong antigenic determinants when fixed to a large carrier molecule. The fact that **4** given to rodents produced an antibody so active against **5** begs the question regarding the antibodies' potential in controlling the course of a vibrio infection in an animal model. We believe the data are further in keeping with the idea that covalently linking siderophore analogues to siderophore bacterial outer membrane receptors[38] or to defined siderophore outer membrane receptor c-terminal peptide fragments represents a credible target for vaccine development. Although there are many potential pitfalls,

nevertheless, because of the above data, we feel compelled to look at this approach. This will be the subject of a future manuscript.

Experimental Section

Biological Materials and Methods. The animal-related protocols were approved by the University of Florida Institutional Animal Care and Use Committee. Three female Balb/c ByJ mice (6−7 weeks old) were purchased from The Jackson Laboratory (Bar Harbor, ME). TiterMax Adjuvant was obtained from Sigma (St. Louis, MO). ELISA plates (MaxiSorp) were purchased from Nalge Nunc International Co. (Naperville, IL). An automatic microplate washer (model EL404, Bio-Tek Instruments, Inc., Winooski, VT) and microplate reader (Spectromax Plus 384, Molecular Devices, Union City, CA) were utilized. The rabbit antimouse IgG (whole molecule), goat antimouse IgG (γ-chain specific), and goat antimouse IgM (μ-chain specific) antibodies were purchased from Sigma (St. Louis, MO). Dulbecco's modified Eagle's medium (HyClone) was obtained from Thermo Fisher Scientific (Waltham, MA). Hybridoma plates were incubated in a Forma Scientific Incubator, model 3154 (Marietta, GA). A MycoAlert Kit (Lonza, Allendale, NJ) was used to assess potential mycoplasma contamination. Monoclonal antibodies were produced using hybridoma production media, BD Cell Mab Medium, Quantum Yield (BD Biosciences, San Jose, CA), supplemented with 10% low IgG fetal bovine serum (HyClone, Thermo Fisher Scientific, Waltham, MA) in CELLine CL 350 flasks (Sartorius Stedim, New York, NY). Amicon Ultra-15 centrifugal filters with a 30 kDa cutoff were obtained from Millipore (Billerica, MA). Male Sprague−Dawley rats (400−450 g) were procured from Harlan Sprague−Dawley (Indianapolis, IN). Cremophor RH-40 was provided by BASF (Parsippany, NJ). An atomic absorption spectrometer, Perkin-Elmer model 5100 PC (Norwalk, CT), was used to determine the iron content of the rat bile and urine samples.

Monoclonal Antibody Production: Immunization. To produce antibodies to small molecules in animals, conjugation to larger carrier proteins (e.g., **27** or **28**) is generally required. Compound **6** was conjugated with **27** using a linker to prepare **4**, which was mixed with an adjuvant and used as an antigen to immunize two mice. One mouse (M1) received 50 μg of **4** per sc injection, and the other mouse (M2) received 100 μg of **4** per sc injection. The mice were given a second immunization of **4** at the same doses four weeks later.

Noncompetitive Binding ELISA Procedure. The method followed the approach of Kao and Klein.[60] Briefly, the assay involved coating a potential antigen (50 μL/well) on the ELISA plates, utilizing solutions of antigens ranging in concentration from 1 to 40 μg/mL. The antigens (a) BSA−VIB conjugate (**5**), (b) BSA−cysteine conjugate (**30**), (c) vibriobactin thiol (**6**), (d) vibriobactin disulfide (**26**), (e) vibriobactin disulfide−iron complex (**34**), (f) vibriobactin (**3**), and (g) vibriobactin iron complex (**33**) were diluted in blocking buffer (1% BSA in PBS with 0.02% azide). Normal mouse sera (NMS) or medium served as negative controls. Polyclonal serum from an immunized mouse (M2) in a 1:1000 dilution or hybridoma supernatant (Tables 4 and 5) were used as positive controls.

The plates were allowed to incubate overnight at 4 °C. An ELISA wash buffer (EWB) containing PBS with 0.02% azide and 0.5% Tween-20 was used to wash the plates. The plates were washed 4 times (300 μL/wash) using an automatic microplate washer. The wells were then blocked with 1% BSA in PBS with 0.02% azide for 1 h at room temperature and washed again. A 50 μL aliquot of diluted polyclonal mouse serum (1:200−1:25600), undiluted hybridoma supernatant, or purified mAb (0.11 μg protein/mL) was added to each well. The plates for this and each subsequent step of the ELISA were incubated with gentle agitation for 1 h at room temperature. The plates were then washed 4 times as above, and rabbit antimouse IgG (whole molecule), conjugated to alkaline phosphatase, was added (50 μL/well); the IgG antibody was diluted (1:1000) in BSA-blocking buffer. The plates were washed 4 times as above, and *p*-nitrophenyl phosphate at a concentration of 1.0 mg/mL, 100 μL/well, was added. The plates were read using an ELISA plate reader at 405 nm, tracking the absorbance (OD) of the yellow water-soluble product, *p*-nitrophenol. A positive response was considered a test well with a *p*-nitrophenol OD value 3 times greater than that of the negative control.

The class of antibody (IgG or IgM) of the hybridoma supernatant (Table 3) or the clone supernatant (Table 5) was determined by an ELISA, replacing the rabbit antimouse IgG (whole molecule) with goat antimouse IgG (γ-chain specific) or goat antimouse IgM (μ-chain specific) at a dilution of 1:4000 (50 μL/well).

Competitive Binding ELISA Procedure. Competitive binding ELISAs were performed on (1) serum from immunized mice that contained polyclonal antibodies and (2) purified mAb derived from the cloning of 5A6−2D5 and 2F10−1A9. Medium was used as a negative control, while **27** (10 μg/mL, 50 μL/well) served as a positive control for the competitive binding ELISA of the polyclonal serum (Table 2) and purified mAb (Table 6). Two types of plates were utilized: a conical bottom polypropylene plate was used for the incubation of the antibody−antigen mixture, whereas a 96-well MaxiSorp plate was used for the ELISA.

In brief, the polypropylene incubation plate was blocked with 300 μL of blocking buffer (1% BSA in PBS with 0.02% azide) and was allowed to incubate overnight at 4 °C. The following day, the blocking buffer was removed (flicked) from the plate, and the plate was blotted on a paper towel. A 96-well ELISA plate was coated with antigen **5** (10 μg/mL, 50 μL/well) that had been diluted in PBS with 0.02% azide. After incubation overnight at 4 °C, the plate was washed 4 times (300 μL/wash) as described above, blocked with 300 μL of blocking buffer for 1 h, and washed again.

Antigens d−g were diluted in blocking buffer in microcentrifuge tubes at antigen concentrations ranging from 0 to 250 μg/mL. The diluted antigens (50 μL/well) were transferred from the microcentrifuge tubes to the polypropylene incubation plate that had been blocked and washed. A 50 μL aliquot of the diluted polyclonal mouse serum (1:10000 dilution) or mAb (0.11 μg protein/mL) was added to the incubation plate wells containing the diluted antigens. The polypropylene plate was then incubated on a rocking platform for 2 h at room temperature, allowing time for the antigen−antibody complexes to form.

A portion of the antigen/antibody mixture (50 μL) was transferred from the polypropylene incubation plate to the **5**-coated ELISA plate that had been blocked and washed. The ELISA plate was incubated with gentle agitation for 1 h at room temperature and was washed 4 times with the EWB. Rabbit antimouse IgG antibodies conjugated to alkaline phosphatase were added (50 μL/well); the IgG antibody was diluted (1:1000) in 1% BSA-blocking buffer. After 1 h, the ELISA plate was washed 4 times with the EWB to remove any unreacted IgG antibodies. *p*-Nitrophenyl phosphate substrate (1.0 mg/mL, 100 μL/well) was added. The ELISA plate was allowed to incubate with gentle agitation for 1 h at room temperature and was read at 405 nm, tracking the OD of the yellow water-soluble product, *p*-nitrophenol. Reduction in the OD value of a test well compared to the positive control reflects the effectiveness of the competitor binding to the antibody.

Cell Fusion−Hybridoma Formation. Four months after the second immunization, 4 days before fusion, a mouse (M2) was given a prefusion booster of 100 μg of **4** without adjuvant. This final immunization was given intraperitoneally (ip). On the day of fusion, the mouse was anesthetized, exsanguinated, and euthanized. The spleen was removed and washed with Dulbecco's modified Eagle's medium to remove the antibody-forming cells. The medium was supplemented with 10% equine serum and 1× antibiotic−antimycotic (per mL: 100 IU of penicillin, 0.10 mg of streptomycin, 0.25 μg of amphotericin B, and 50 μg of gentamycin). The fusion was performed by the procedures described in Simrell et al.[61] except that the myeloma cell line used was Sp2/0 (a murine myeloma aminopterin-resistant cell line with a defect in purine metabolism). Spleen cells were mixed with myeloma cells at a 7:1 ratio. The fusion was performed with 50% polyethylene glycol 1500 followed by a controlled dilution with media. A centrifugation step

(1500−1800 rpm for 8 min) was performed to pellet the fused cells. The pellet was resuspended in Dulbecco's modified Eagle's medium-high glucose, supplemented with 20% equine serum, 25% Sp2/0 myeloma conditioned medium and 1× hypoxanthine, aminopterin, thymidine (HAT) and was seeded in five 96-well plates at 2.8×10^5 cells per well. The plates were incubated at 37 °C, with a CO_2 concentration of 7%.

Eleven days postfusion, supernatants from the resulting HAT-resistant hybridomas were subjected to a primary ELISA screening to detect if the cells were secreting antibodies against **5**. Cells from 51 wells that were positive in the primary screening against **5** were transferred to three 24-well plates and further incubated. The supernatant was assessed again 1 week later in a secondary ELISA screening against **5**, **35**, and **30** (Table 3). The hybridomas that were **5** and **35** positive and **30** negative were further tested as described above to determine the class of antibody, IgG or IgM (Table 3).

Cloning of Antibody-Producing Hybridomas. Two of the most promising hybridomas, 5A6 and 2F10, were cloned. Cells from the hybridomas were diluted to a concentration of one or two cells per well and were seeded in eight 96-well plates (four plates each for 5A6 and 2F10) over a feeder layer of irradiated 3T3 mouse fibroblasts. After incubation for 4 days, the plates were scanned microscopically and were scored for single colony and multiple colony wells. For the 5A6 cell line, 96 single colony wells and 60 multiple colony wells were found, whereas the 2F10 cell line presented 120 single colony wells and 47 multiple colony wells. Ten days after seeding, the supernatants from all 323 wells that contained cells underwent screening via ELISA against **5**.

Supernatants from the single colony wells of 5A6 were not very active against **5** (data not shown). Because of this, the four most **5** positive multiple colony wells of 5A6 were pooled, diluted, and replated as single cells in four 96-well plates. Ten days after this recloning, the 10 single colony wells with the strongest ELISA positives (primary) against **5** were chosen (Table 4) and cultured in a 24-well plate. After incubation for an additional 5 days, the supernatant was tested again (secondary) via ELISA against **5**, **35**, and **30**. All 10 clones were highly active against **5** and **35** and showed little activity toward **30** (Table 4).

Recloning of the 2F10 hybridoma was unnecessary. The 10 single colony wells with the strongest ELISA response against **5** from the four 96-well plates were transferred to a 24-well plate. After incubation for an additional 5 days, the supernatants were tested against **5**, **35**, and **30**. Two clones from 2F10 (2F10−1A9 and 2F10−2A3), as well as two clones from 5A6 (5A6−2D5 and 5A6−1G8), were chosen for further evaluation. Cell lines 5A6-1G8, 5A6-2D5, 2F10-2A3, and 2F10-1A9 were tested for mycoplasma contamination and were found negative (Table 5). Multiple stocks from each of the four cell lines were frozen.

Production and Purification of Monoclonal Antibodies. 5A6−2D5 or 2F10−1A9 cloned hybridoma cells were grown in hybridoma production media supplemented with 10% low IgG fetal bovine serum in CELLine CL 350 flasks. The flasks were incubated at 37 °C with a CO_2 concentration of 7%. One harvest per week was taken for 3 weeks. The cells were centrifuged at 2000 rpm for 15 min, and the resulting supernatant was collected and purified by circulating through a 5 mL protein G Sepharose 4B column. The supernatant recirculated through the column for 90 min (∼23 passes). The column was then rinsed with PBS (70−150 mL). The antibodies were eluted using 0.1 M glycine, pH 2.8. Ten fractions of 3 mL each were collected. The eluted fractions were neutralized with 2.0 M Tris, pH 9.0. Absorbance was measured at 280 nm. Fractions with the highest absorbance readings were pooled, desalted, and concentrated using Amicon Ultra-15 centrifugal filters with a 30 kDa cutoff. The concentrated, purified monoclonal antibodies were recovered in a final volume of 0.6 mL in PBS. The protein concentration of the purified mAb were measured spectrophotometrically at 280 nm. Most mammalian antibodies (i.e., immunoglobulins) have protein extinction coefficients ($\varepsilon_{percent}$) in the range of 12−15.[64] The final protein concentration of the purified IgG antibody was estimated assuming a protein extinction coefficient of 14. For an IgG antibody with a molecular weight of approximately 150000, this corresponds to a molar extinction coefficient (ε) of 210000 M^{-1} cm^{-1}.

Iron Clearance in Non-Iron-Overloaded, Bile-Duct Cannulated Rats. Four rats were subjected to bile duct-cannulation as previously described.[62,63] The rats were given **3** sc at a dose of 75 μmol/kg. The drug was solubilized in 40% Cremophor RH-40/water. Bile samples were collected from the rats at 3 h intervals for 48 h. The urine samples were taken at 24 h intervals. Sample collection and handling are as previously described.[62,63] The iron content of the bile and urine were assessed by atomic absorption spectroscopy. Iron clearing efficiency was calculated as set forth elsewhere.[65] The theoretical iron output of the chelator was generated on the basis of a 1:1 vibriobactin−iron complex.[48]

Synthetic Materials and Methods. Reagents were purchased from Aldrich Chemical Co. (Milwaukee, WI). Fisher Optima-grade solvents were routinely used, and DMF was distilled. Organic extracts were dried with sodium sulfate and then filtered. Distilled solvents and glassware that had been presoaked in 3 N HCl for 15 min were employed in reactions involving chelators. Silica gel 70-230 from Fisher Scientific was utilized for column chromatography, and silica gel 40-63 from SiliCycle, Inc. (Quebec City, Quebec, Canada) was used for flash column chromatography. Sephadex LH-20 was obtained from Amersham Biosciences (Piscataway, NJ). An ICP-MS X 0675, manufactured by Thermo Electron Corporation (England), was used for the determination of the iron content of selected solutions/compounds. Derivatized OVA or BSA protein containing maleimide moieties **27** and **28**, respectively, were obtained from Pierce (Rockford, IL).[66] NMR spectra were obtained at 400 MHz (^{1}H) or 100 MHz (^{13}C) on a Varian Mercury-400BB. Chemical shifts (δ) for ^{1}H spectra are given in parts per million downfield from tetramethylsilane for organic solvents ($CDCl_3$ not indicated) or sodium 3-(trimethylsilyl)propionate-2,2,3,3-d_4 for D_2O. Chemical shifts (δ) for ^{13}C spectra are given in parts per million referenced to 1,4-dioxane (δ 67.19) in D_2O or to the residual solvent resonance in $CDCl_3$ (δ 77.16). Coupling constants (J) are in hertz. The base peaks are reported for the high resolution mass spectra. Elemental analyses were performed by Atlantic Microlabs (Norcross, GA) and were within ±0.4% of the calculated values.

OVA−VIB (4) and BSA−VIB (5). Derivatized proteins **27**[66] or **28**[66] (2 mg each) were dissolved in the conjugation buffer (100 μL) and incubated with a freshly prepared solution of **6** (2 mg in 200 μL of 50% aqueous DMSO) for 8 h. Unreacted maleimide was capped by conjugating it further with cysteine (2 mg in 50 μL degassed water) for 8 h. After incubation, **4** and **5** respectively were purified on a dextran desalting column (5 mL), eluting with 30% DMSO/purification buffer. Fractions (0.5 mL) were collected, and the OD was measured at 280 nm. Positive fractions of each conjugate were pooled, and the protein concentration of each conjugate was estimated by a Coomassie assay.[58]

1-(2,3-Dihydroxybenzoyl)-5,9-bis[[(4*S*,5*R*)-2-(2,3-dihydroxyphenyl)-4,5-dihydro-5-methyl-4-oxazolyl]carbonyl]-14-(3-mercaptopropanoyl)-1,5,9,14-tetraazatetradecane (6). Palladium black (0.127 g) was added to a solution of **26** (0.231 g, 0.133 mmol) in anhydrous degassed EtOH (5 mL), and the mixture was stirred under H_2 at 45 psi for 24 h. After filtration through Celite and washing the solids with degassed EtOH (2 × 5 mL), the filtrate was concentrated in vacuo to afford 0.137 g (60%) of **6** as a brown solid: ^{1}H NMR δ 1.35−1.75 (m, 10 H), 1.8−2.2 (m, 4 H), 2.47−2.59 (m, 2 H), 2.82−2.91 (m, 2 H), 3.02−3.91 (m, 12 H), 4.72−5.0 (m, 2 H), 5.21−5.36 (m, 2 H), 6.58−6.77 (m, 3 H), 6.84−7.2 (m, 3 H), 7.24−7.8 (m, 3 H); HRMS *m*/*z* calcd for $C_{42}H_{53}N_6O_{12}S$, 865.3358 (M + H); found, 865.3466.

***N*^{1}-(4-Hydroxybutyl)-*N*^{1},*N*^{4},*N*^{7}-tris(*tert*-butoxycarbonyl)norspermidine (9).** 4-Chloro-1-butanol (16.5 g, 0.150 mol) was introduced to a mixture of **7** (39.4 g, 0.300 mol), KI (2.475 g, 15.0 mmol), and K_2CO_3 (10.5 g, 75.0 mmol) in anhydrous 1-butanol (375 mL). The mixture was stirred at 125 °C for 24 h, slowly cooled to room temperature, filtered, and concentrated under vacuum to afford **8** as a viscous oil, which was dissolved in 50% aqueous THF (500 mL). Di-*tert*-butyl dicarbonate (130.8 g, 0.600 mol) in

THF (100 mL) was added with continuous stirring. After 16 h, volatiles were removed, and the residue was dissolved in H_2O (300 mL) and extracted with EtOAc (200 mL, 3 × 100 mL). The combined organic layers were washed with 0.5 M citric acid (100 mL), H_2O (100 mL), and saturated NaCl (100 mL) and were concentrated under reduced pressure. Column chromatography using 49:49:2 hexanes/EtOAc/CH_3OH provided 31.73 g (42%) of **9** as a viscous colorless oil. ^{1}H NMR δ 1.44, 1.45, and 1.46 (3 s, 27 H), 1.5−1.8 (m, 9 H), 3.02−3.34 (m, 10 H), 3.67 (t, 2 H, J = 5.9), 4.78 and 5.27 (2 br s, 1 H); ^{13}C NMR δ 25.20, 27.84, 28.57, 28.60, 28.61, 29.82, 37.72, 44.10, 45.01, 47.01, 62.57, 79.57, 155.75, 156.16, 174.84; HRMS *m*/*z* calcd for $C_{25}H_{50}N_3O_7$, 504.3648 (M + H); found, 504.3640. Anal. ($C_{25}H_{49}N_3O_7$) C, H, N.

***N*^{1}-[4-(Tosyloxy)butyl]-*N*^{1},*N*^{4},*N*^{7}-tris(*tert*-butoxycarbonyl)norspermidine (10). 10** was prepared from **9** by our previous reaction conditions.[55] HRMS *m*/*z* calcd for $C_{32}H_{56}N_3O_9S$, 657.3659 (M + H); found, 657.3672. Anal. ($C_{32}H_{55}N_3O_9S$) C, H, N.

***N*^{1}-[4-(Phthalimido)butyl]-*N*^{1},*N*^{4},*N*^{7}-tris(*tert*-butoxycarbonyl)-norspermidine (11).** Potassium phthalimide (1.138 g, 6.15 mmol) was added to **10** (2.70 g, 4.10 mmol) in DMF (50 mL), and the reaction mixture was heated at 90 °C for 48 h. Solvent was removed in vacuo, and the residue was treated with H_2O (50 mL) and extracted with $CHCl_3$ (3 × 50 mL). The combined organic phase was washed with saturated NaCl and concentrated under reduced pressure. Column chromatography with 20% EtOAc/$CHCl_3$ generated 1.84 g (71%) of **11**: ^{1}H NMR δ 1.43−1.45 (3 s, 27 H), 1.52−1.76 (m, 8 H), 3.06−3.29 (m, 10 H), 3.71 (t, 2 H, J = 6.8), 7.70−7.73 (m, 2 H), 7.83−7.87 (m, 2 H); ^{13}C NMR δ 25.98, 27.46, 28.48, 29.49, 37.40, 37.60, 43.71, 44.87, 46.52, 78.88, 79.43, 79.65, 123.25, 123.41, 132.10, 133.99, 134.11, 155.45, 156.03, 168.41. HRMS *m*/*z* calcd for $C_{33}H_{53}N_4O_8$, 633.3858 (M + H); found, 633.3920. Anal. ($C_{33}H_{52}N_4O_8$) C, H, N.

***N*^{1}-[4-(Phthalimido)butyl]norspermidine Tris(trifluoroacetate) (12).** TFA (25 mL) was added to **11** (3.46 g, 5.47 mmol) in CH_2Cl_2 (25 mL) with ice bath cooling, and the solution was stirred for 1 h at 0 °C and 1 h at room temperature. After removal of volatiles in vacuo, the residue was treated with toluene and dried by high vacuum to give 3.69 g (quantitative) of **12** as a white solid: ^{1}H NMR (D_2O) δ 1.72−1.75 (m, 4 H), 2.05−2.15 (m, 4 H), 3.08−3.19 (m, 10 H), 3.71 (t, 2 H, J = 6.4), 7.81−7.87 (m, 4 H); ^{13}C NMR δ (D_2O) 23.24, 23.56, 24.37, 25.47, 37.10, 37.53, 44.90, 45.20, 45.29, 47.79, 123.91, 131.71, 135.37, 171.17; HRMS *m*/*z* calcd for $C_{18}H_{29}N_4O_2$ 333.2285 (M + H, free amine); found, 333.2324. Anal. ($C_{24}H_{31}F_9N_4O_8 \cdot 1.5H_2O$) C, H, N.

***N*^{1}-(2,3-Dimethoxybenzoyl)-*N*^{7}-[4-(phthalimido)butyl]norspermidine (13).** CDI (0.563 g, 3.48 mmol) was added to a solution of 2,3-dimethoxybenzoic acid (0.633 g, 3.48 mmol) in CH_2Cl_2 (5 mL). After being stirred for 1 h, the solution was cooled to 0 °C and was added to a suspension of **12** (2.82 g, 4.18 mmol) and NEt_3 (2.46 g, 24.4 mmol) in CH_2Cl_2 (30 mL). The reaction mixture was stirred for 15 h at room temperature, diluted with CH_2Cl_2 (100 mL), and washed with 8% $NaHCO_3$ (50 mL). The organic phase was concentrated in vacuo, and the residue was subjected to flash chromatography, eluting with 5% concentrated NH_4OH/MeOH to afford 1.20 g (70%) of **13** as a colorless oil: ^{1}H NMR δ 1.48−1.57 (m, 2 H), 1.62−1.85 (m, 6 H), 2.61−2.73 (m, 8 H), 3.53 (q, 2 H, J = 6.0), 3.70 (t, 2 H, J = 7.6), 3.88 (s, 3 H), 3.89 (s, 3 H), 7.03 (dd, 1 H, J = 8.0, 1.6), 7.14 (t, 1 H, J = 8.0), 7.64 (dd, 1 H, J = 8.0, 1.6), 7.69−7.71 (m, 2 H), 7.82−7.84 (m, 2 H), 8.15 (br, 1 H, J = 7.2); HRMS *m*/*z* calcd for $C_{27}H_{37}N_4O_5$, 497.2765 (M + H); found, 497.2671. Anal. ($C_{27}H_{36}N_4O_5$) C, H, N.

***N*^{4},*N*^{7}-Bis[(*N*-*tert*-butoxycarbonyl-L-threonyl]-*N*^{1}-(2,3-dimethoxybenzoyl)-*N*^{7}-[4-(phthalimido)butyl]norspermidine (14).** A solution of freshly prepared *N*-*tert*-butoxycarbonyl-L-threonine *N*-hydroxysuccinimide ester[56] (4.17 g, 13.2 mmol) in DMF (20 mL) was added to a solution of **13** (2.2 g, 4.4 mmol) in DMF (20 mL). After the mixture was stirred for 72 h, the solvent was removed under vacuum and the residue was taken up in $CHCl_3$ (50 mL). The organic layer was washed with 5% $NaHCO_3$ (3 × 50 mL), H_2O (50 mL), and saturated NaCl (50 mL) and was concentrated in vacuo. Flash chromatography, eluting with 10% EtOH/EtOAc, furnished 2.17 g (55%) of **14** as a white foam: ^{1}H NMR δ 1.14−1.22 (m, 6 H), 1.38−1.46 (m, 18 H), 1.54−2.02 (m, 8 H), 2.90−3.61 (m, 10 H), 3.68−3.76 (m, 2 H), 3.89 (s, 3 H), 3.91 (s, 3 H), 3.98−4.14 (m, 2 H), 5.44−5.68 (m, 2 H), 7.04 (d, 1 H, J = 8.4), 7.14 (d, 1 H, J = 8.0), 7.62−7.67 (m, 1 H), 7.70−7.72 (m, 2 H), 7.84−7.86 (m, 2 H); HRMS *m*/*z* calcd for $C_{45}H_{67}N_6O_{13}$, 899.4767 (M + H); found, 899.4783. Anal. ($C_{45}H_{66}N_6O_{13}$) C, H, N.

***N*^{4},*N*^{8}-Bis[(*N*-*tert*-butoxycarbonyl-L-threonyl]-*N*^{1}-(2,3-dimethoxybenzoyl)thermospermine (15).** Hydrazine hydrate (5 mL) was added to a solution of **14** (0.350 g, 0.389 mmol) in EtOH (10 mL), and the reaction mixture was stirred at room temperature for 16 h. Solid was filtered, and the filtrate was concentrated in vacuo. The residue was taken up in 1 N NaOH (10 mL) and extracted with $CHCl_3$ (3 × 10 mL), and organic extracts were concentrated. Flash chromatography, eluting with 1% concentrated NH_4OH/MeOH, gave 195 mg (65%) of **15** as a viscous solid: ^{1}H NMR δ 1.14−1.22 (m, 6 H), 1.38−1.46 (m, 18 H), 1.54−2.02 (m, 8 H), 2.68−2.76 (m, 2 H), 2.90−3.61 (m, 10 H), 3.89 (s, 3 H), 3.91−3.94 (m, 3 H), 3.98−4.14 (m, 2 H), 4.44−4.62 (m, 2 H), 5.46−5.64 (m, 2 H), 7.04 (d, 1 H, J = 8.4), 7.14 (t, 1 H, J = 8.0), 7.62−7.67 (m, 1 H); HRMS *m*/*z* calcd for $C_{37}H_{65}N_6O_{11}$, 769.4713 (M + H); found, 769.4709. Anal. ($C_{37}H_{64}N_6O_{11}$) C, H, N.

1,36-Bis(2,3-dimethoxybenzoyl)-15,22-dioxo-18,19-dithia-1,5,9,14,23,28,32,36-octaaza-5,9,28,32-tetrakis[(*N*-*tert*-butoxycarbonyl-L-threonyl]hexatriacontane (16). CDI (0.10 g, 0.65 mmol) was added to a solution of 3,3′-dithiopropionic acid (0.06 g, 0.32 mmol) in CH_2Cl_2 (2 mL). After the mixture was stirred for 2 h, a solution of **15** (0.60 g, 0.78 mmol) in CH_2Cl_2 (5 mL) was added to the reaction mixture. The solution was stirred for 15 h at room temperature and was diluted with CH_2Cl_2 (25 mL). The organic layer was washed with 1 N NaOH (15 mL) and saturated NaCl (15 mL) and was concentrated in vacuo. Flash chromatography using 15% EtOH/$CHCl_3$ generated 0.218 g (40%) of **16** as a pale-brown solid: ^{1}H NMR δ 1.10−1.25 (m, 12 H), 1.29−1.50 (m, 36 H), 1.52−2.05 (m, 16 H), 2.50−2.65 (m, 4 H), 2.90−3.08 (m, 4 H), 3.09 −3.60 (m, 24 H), 3.85−3.98 (m, 12 H), 3.99−4.60 (m, 8 H), 5.40−5.65 (m, 4 H), 6.98−7.15 (m, 2 H), 7.18−7.20 (m, 2 H), 7.60−7.69 (m, 2 H); HRMS *m*/*z* calcd for $C_{80}H_{135}N_{12}O_{24}S_2$, 1711.9155 (M + H); found, 1711.9170.

1-(2,3-Dihydroxybenzoyl)-5,9-bis[(*N*-*tert*-butoxycarbonyl-L-threonyl]-14-(3-mercaptopropanoyl)-1,5,9,14-tetraazatetradecane Dihydrobromide (17). Boron tribromide in CH_2Cl_2 (1 M, 7.56 mL, 7.56 mmol) was added to a mixture of **16** (340 mg, 0.199 mmol) in CH_2Cl_2 (20 mL) at −78 °C, and after being stirred for 1 h, the reaction mixture was warmed to room temperature and was stirred for 15 h. The reaction mixture was quenched cautiously at 0 °C with H_2O (10 mL) and was stirred for 2 h. The aqueous layer was extracted with CH_2Cl_2 (20 mL) and was concentrated in vacuo, and the residue was subjected to a Sephadex LH-20 column, eluting with 40% EtOH/toluene to give 115 mg (73%) of **17** as a white solid: ^{1}H NMR (D_2O) δ 1.15−1.25 (m, 6 H), 1.46−2.01 (m, 8 H), 2.56−2.63 (m, 2 H), 2.94−3.00 (m, 2 H), 3.03−3.68 (m, 12 H), 4.04−4.20 (m, 2 H), 4.24−4.39 (m, 2 H), 6.83 (t, 1 H, J = 8.4), 7.15 (d, 1 H, J = 8.0), 7.30 (d, 1 H, J = 7.6); HRMS *m*/*z* calcd for $C_{28}H_{49}N_6O_8S$, 629.3333 (M + H, free amine); found, 629.3329. Anal. ($C_{28}H_{50}Br_2N_6O_8S \cdot H_2O$) C, H, N.

4-Methoxybenzyl 2,3-Bis(4-methoxybenzyloxy)benzoate (19). Sodium hydride (60%, 4.69 g, 0.117 mol) was added in portions to **18** (5.47 g, 35.5 mmol) in DMF (150 mL) with ice bath cooling, and the mixture was stirred at 0 °C for 45 min and at room temperature for 1 h. A solution of 4-methoxybenzyl bromide (25.0 g, 0.124 mol) in DMF (50 mL) was added to the reaction mixture over 30 min. After the mixture was stirred for 20 h, quenching with H_2O (30 mL) at 0 °C was performed, and solvents were removed under high vacuum. The concentrate was dissolved in EtOAc (200 mL), which was washed with H_2O (100 mL) and saturated NaCl (100 mL); solvent was removed in vacuo. Flash chromatography, eluting with 5:1 hexanes/EtOAc, gave 11.33 g (62%) of **19** as a white solid, mp 108 °C: ^{1}H NMR δ 3.77 (s, 3 H), 3.79 (s, 3 H), 3.81 (s, 3 H), 4.95 (s, 2 H), 5.03 (s, 2 H), 5.25 (s, 2

H), 6.76 (d, 2 H, $J = 8.8$), 6.86 (d, 2 H, $J = 8.8$), 6.89 (d, 2 H, $J = 8.4$), 7.04 (t, 1 H, $J = 7.8$), 7.11 (dd, 1 H, $J = 8.0, 2.0$), 7.18 (d, 2 H, $J = 8.8$), 7.33−7.36 (m, 5 H); ^{13}C NMR δ 55.32, 55.37, 55.40, 66.81, 71.20, 75.31, 112.97, 113.61, 114.02, 118.16, 123.93, 127.08, 128.19, 128.75, 129.51, 129.73, 130.31, 130.41, 148.43, 152.95, 159.43, 159.62, 159.70, 166.44; HRMS *m/z* calcd for $C_{31}H_{30}NaO_7$, 537.1889 (M + Na); found, 537.1884.

2,3-Bis(4-methoxybenzyloxy)benzoic Acid (20). A solution of **19** (8.60 g, 16.71 mmol) in dioxane (84 mL) and 2 N NaOH (42 mL) was stirred for 24 h at room temperature. The reaction mixture was concentrated in vacuo. The residue was stirred with H_2O (100 mL) and then acidified to pH 2 with 1 N HCl. The white solid was filtered, washed with hexane, and recrystallized from EtOAc/hexanes to generate 5.93 g (90%) of **20** as a white crystalline solid, mp 129 °C: ^{1}H NMR δ 3.8 (s, 3 H), 3.85 (s, 3 H), 5.12 (s, 2 H), 5.20 (s, 2 H), 6.83 (d, 2 H, $J = 8.8$), 6.96 (d, 2 H, $J = 9.2$), 7.18 (t, 2 H, $J = 8.0$), 7.22−7.27 (m, 2 H), 7.41 (d, 2 H, $J = 8.4$), 7.73 (dd, 1 H, $J = 1.2, 8.0$); ^{13}C NMR δ 55.36, 55.37, 55.44, 55.46, 71.42, 114.26, 119.12, 123.04, 124.37, 125.00, 126.87, 128.02, 129.73, 131.21, 147.17, 151.45, 159.94, 160.44, 165.45; HRMS *m/z* calcd for $C_{23}H_{22}NaO_6$, 417.1332 (M + Na); found, 417.1332.

***N*^{1}-[2,3-Bis(4-methoxybenzyloxy)benzoyl]-*N*^{7}-[4-(phthalimido)butyl]norspermidine (21).** CDI (0.239 g, 1.48 mmol) was added to a solution of **20** (0.583 g, 1.48 mmol) in CH_2Cl_2 (2 mL). After being stirred for 1 h, the solution was cooled to 0 °C and added to a suspension of **12** (1.0 g, 1.48 mmol) and NEt_3 (1.05 g, 10.4 mmol) in CH_2Cl_2 (2 mL) at 0 °C. The solution was stirred for 15 h at room temperature and was diluted with CH_2Cl_2 (50 mL). The reaction mixture was washed with 8% $NaHCO_3$ (25 mL) and was concentrated. Flash chromatography, eluting with 5% concentrated NH_4OH/MeOH, afforded 0.597 g (57%) of **21** as a colorless oil: ^{1}H NMR δ 1.48−1.72 (m, 8 H), 2.52−2.63 (m, 8 H), 3.36 (q, 2 H, $J = 6.0$), 3.69 (t, 2 H, $J = 7.2$), 3.80 (s, 3 H), 3.84 (s, 3 H), 4.98 (s, 2 H), 5.07 (s, 2 H), 6.83 (d, 2 H, $J = 8.8$), 6.93 (d, 2 H, $J = 8.4$), 7.13 (d, 2 H, $J = 4.8$), 7.23 (m, 3 H), 7.4 (d, 2 H, $J = 8.4$), 7.68−7.7 (m, 2 H), 7.81−7.83 (m, 2 H), 8.12 (t, 1 H, $J = 7.2$); HRMS *m/z* calcd for $C_{41}H_{49}N_4O_7$, 709.3596 (M + H); found, 709.3611. Anal. ($C_{41}H_{48}N_4O_7$) C, H, N.

***N*^{4},*N*^{7}-Bis[(*N*-*tert*-butoxycarbonyl-L-threonyl]-*N*^{1}-[2,3-bis(4-methoxybenzyloxy)benzoyl]-*N*^{7}-[4-(phthalimido)butyl]norspermidine (22).** A solution of freshly prepared *N*-*tert*-butoxycarbonyl-L-threonine *N*-hydroxysuccinimide ester[56] (1.12 g, 3.54 mmol) in DMF (10 mL) was added to a solution of **21** (1.0 g, 1.41 mmol) in DMF (10 mL). After the mixture was stirred for 72 h at 40 °C, the solvent was removed under vacuum, and the residue was taken up in $CHCl_3$ (50 mL). The organic layer was washed with aqueous 5% $NaHCO_3$ (3 × 50 mL), H_2O (50 mL), saturated NaCl (50 mL) and was concentrated in vacuo. Flash chromatography, eluting with 10% EtOH/EtOAc, afforded 0.945 g (60%) of **22** as a white foam: ^{1}H NMR δ 1.14−1.21 (m, 6 H), 1.37−1.49 (m, 18 H), 1.52−1.8 (m, 8 H), 3.10−3.60 (m, 10 H), 3.68−3.74 (m, 2 H), 3.79−3.81 (m, 3 H), 3.84 (s, 3 H), 3.97−4.11 (m, 2 H), 4.32−4.60 (m, 2 H), 5.02 (s, 2 H), 5.07 (s, 2 H), 5.44−5.62 (m, 2 H) 6.82−6.86 (m, 2 H), 6.93 (d, 2 H, $J = 8.4$), 7.11−7.13 (m, 2 H), 7.22−7.26 (m, 3 H), 7.39 (d, 2 H, $J = 8.4$), 7.69−7.72 (m, 2 H), 7.81−7.85 (m, 2 H), 8.02 (br s, 1 H); HRMS *m/z* calcd for $C_{59}H_{79}N_6O_{15}$, 1111.5598 (M + H); found, 1111.5650. Anal. ($C_{59}H_{78}N_6O_{15}$) C, H, N.

***N*^{4},*N*^{8}-Bis[(*N*-*tert*-butoxycarbonyl-L-threonyl]-*N*^{1}-[2,3-bis(4-methoxybenzyloxy)benzoyl]thermospermine (23).** Hydrazine hydrate (5 mL) was added to a solution of **22** (250 mg, 0.225 mmol) in EtOH (10 mL), and the reaction mixture was stirred at room temperature for 16 h. Solid was filtered, and the filtrate was concentrated under high vacuum. The residue was taken up in 1 N NaOH (10 mL) and extracted with $CHCl_3$ (3 × 10 mL), and organic extracts were concentrated. Flash chromatography, eluting with 1% concentrated NH_4OH/MeOH, afforded 198 mg (90%) of **23** as a white solid: ^{1}H NMR δ 1.11−1.22 (m, 6 H), 1.37−1.43 (m, 18 H), 1.58−2.02 (m, 8 H), 2.71 (q, 2 H, $J = 6.0$), 2.90−3.60 (m, 10 H), 3.80−3.81 (m, 3 H), 3.84 (s, 3 H), 3.98−4.14 (m, 2 H), 4.30−4.60 (m, 2 H), 5.00−5.08 (m, 4 H), 5.42−5.65 (m, 2 H), 6.82−6.86 (m, 2 H), 6.93 (d, 2 H, $J = 8.4$), 7.13−7.19 (m, 2 H), 7.22−7.26 (m, 3 H), 7.4 (d, 2 H, $J = 8.4$); HRMS *m/z* calcd for $C_{51}H_{77}N_6O_{13}$, 981.5543 (M + H); found, 981.5589. Anal. ($C_{51}H_{76}N_6O_{13}$) C, H, N.

1,36-Bis[2,3-bis(4-methoxybenzyloxy)benzoyl]-15,22-dioxo-18,19-dithia-1,5,9,14,23,28,32,36-octaaza-5,9,28,32-tetrakis[(*N*-*tert*-butoxycarbonyl-L-threonyl]hexatriacontane (24). CDI (0.063 g, 0.372 mmol) was added to a solution of 3,3′-dithiopropionic acid (0.039 g, 0.186 mmol) in CH_2Cl_2 (2 mL). After the mixture was stirred for 2 h, a solution of **23** (0.550 g, 0.56 mmol) in CH_2Cl_2 (5 mL) was added followed by NEt_3 (0.025 g, 0.25 mmol). The solution was stirred for 15 h at room temperature and was diluted with CH_2Cl_2 (25 mL). The organic layer was washed with 8% $NaHCO_3$ (20 mL) and saturated NaCl (20 mL) and concentrated in vacuo. Flash chromatography, using 8% $CH_3OH/CHCl_3$, generated 0.238 g (60%) of **24** as a pale-brown solid: ^{1}H NMR δ 1.10−1.23 (m, 12 H), 1.25−1.47 (m, 36 H), 1.48−2.00 (m, 16 H), 2.52−2.70 (m, 4 H), 2.80−3.01 (m, 4 H), 3.07−3.55 (m, 24 H), 3.80−3.81(m, 6 H), 3.83 (s, 6 H), 3.95−4.17 (m, 4 H), 4.27−4.62 (m, 4 H), 5.01−5.04 (m, 4 H), 5.07 (2 s, 4 H), 5.42−5.65 (m, 4 H), 6.82−6.86 (m, 4 H), 6.93 (2 d, 4 H, $J = 8.4$), 7.12−7.18 (m, 4 H), 7.22−7.27 (m, 6 H), 7.4 (d, 4 H, $J = 8.4$); HRMS *m/z* calcd for $C_{108}H_{159}N_{12}O_{28}S_2$ 2137.0859 (M + H), found 2137.0867. Anal. ($C_{108}H_{158}N_{12}O_{28}S_2$) C, H, N.

1,36-Bis(2,3-dihydroxybenzoyl)-15,22-dioxo-18,19-dithia-1,5,9,14,23,28,32,36-octaaza-5,9,28,32-tetrakis(L-threonyl)hexatriacontane Tetrakis(trifluoroacetate) (25). TFA (25 mL) was added to a mixture of **24** (1.16 g, 0.547 mmol) and anisole (5 mL) in CH_2Cl_2 (25 mL) with ice bath cooling, and the solution was stirred for 1 h at 0 °C and 1 h at room temperature. After removal of volatiles in vacuo, the concentrate was subjected to a Sephadex LH-20 column, eluting with 40% EtOH/toluene to give 0.54 g of **25** (60%) as a white solid: ^{1}H NMR (D_2O) δ 1.24−1.30 (m, 12 H), 1.34−1.60 (m, 8 H), 1.74−2.21 (m, 8 H), 2.57−2.66 (m, 4 H), 2.84−2.93 (m, 4 H), 3.0−3.64 (m, 24 H), 4.04−4.20 (m, 4 H), 4.24−4.38 (m, 4 H), 6.80−6.86 (m, 2 H), 7.03−7.07 (m, 2 H), 7.18−7.21 (m, 2 H); HRMS *m/z* calcd for $C_{56}H_{95}N_{12}O_{16}S_2$, 1255.6425 (M + H, free amine); found, 1255.6417. Anal. ($C_{64}H_{98}F_{12}N_{12}O_{24}S_2 \cdot 2.5H_2O$) C, H, N.

1,36-Bis(2,3-dihydroxybenzoyl)-15,22-dioxo-18,19-dithia-1,5,9,14,23,28,32,36-octaaza-5,9,28,32-tetrakis[[(4*S*,5*R*)-2-(2,3-dihydroxyphenyl)-4,5-dihydro-5-methyl-4-oxazolyl]carbonyl]hexatriacontane (26). Ethyl 2,3-dihydroxybenzimidate[34] (0.231 g, 1.27 mmol) was added to a solution of **25** (0.35 g, 0.21 mmol) in anhydrous EtOH (15 mL). The mixture was heated at reflux under N_2 for 36 h and was concentrated in vacuo. Column chromatography on Sephadex LH-20, eluting with 15% EtOH/toluene, afforded 0.072 g (20%) of **26** as a gray solid: ^{1}H NMR δ 1.35−1.75 (m, 20 H), 1.8−2.2 (m, 8 H), 2.47−2.59 (m, 4 H), 2.82−2.91 (m, 4 H), 3.02−3.91 (m, 24 H), 4.72−5.0 (m, 4 H), 5.21−5.36 (m, 4 H), 6.58−6.77 (m, 6 H), 6.84−7.02 (m, 6 H), 7.08−7.24 (m, 6 H); HRMS *m/z* calcd for $C_{84}H_{103}N_{12}O_{24}S_2$, 1728.6669 (M + H); found, 1728.7344. Anal. ($C_{84}H_{102}N_{12}O_{24}S_2$) C, H, N.

BSA−Cysteine Conjugate (30). Maleimide-activated protein **28**[66] (2 mg in 100 μL buffer) and cysteine (2 mg in 200 μL of degassed water) were incubated for 8 h at room temperature. After incubation, **30** was purified on a dextran desalting column, eluting with a purification buffer. Fractions (0.5 mL) were collected, and the OD was measured at 280 nm. Positive fractions were pooled, and protein concentration was estimated by Coomassie assay.[58]

Iron Complex of OVA−VIB Protein Conjugate (31). A 1 mL solution of **4** (1.685 mg/mL) was incubated at pH 7.4 with 1 mM FeNTA (500 μL) at room temperature. After the mixture was incubated for 2 h, excess **1** was added and the mixture again incubated for 2 h. The mixture was subjected to a G-25 Sepharose column, using 30% DMSO/phosphate buffer as an eluting solvent. Fractions (0.5 mL) were collected, and the first colored band (fractions 3−6) was eluted; the OD was checked at 280 nm. Protein-containing fractions were pooled (4 mL) and subjected to ICP-MS for estimation of iron content.

Iron Complexes of Vibriobactin (33) and Vibriobactin Disulfide (34). The iron complexes of compounds **3** and **26** were prepared by the previously reported method.[59]

Acknowledgment. This paper is dedicated to Dr. William R. Weimar in recognition of his many contributions to our research program over the years. The project described was supported by Grant Numbers R37DK049108 (National Institute of Diabetes and Digestive and Kidney Diseases) and R01AI074068 (National Institute of Allergy and Infectious Diseases). The content is solely the responsibility of the authors and does not necessarily represent the official views of the National Institute of Diabetes and Digestive and Kidney Diseases, the National Institute of Allergy and Infectious Diseases, or the National Institutes of Health. We thank Elizabeth M. Nelson for her technical assistance and Miranda E. Coger for her editorial and organizational support. We acknowledge the spectroscopy services in the Chemistry Department, University of Florida, for the mass spectrometry analyses and Diane G. Duke of the Hybridoma Core Laboratory, Interdisciplinary Center for Biotechnology Research, University of Florida, for the ELISA assessments of antibodies against the OVA−VIB conjugate.

Supporting Information Available: Elemental analytical data for synthesized compounds. This material is available free of charge via the Internet at http://pubs.acs.org.

References

(1) Bergeron, R. J.; Brittenham, G. M. *The Development of Iron Chelators for Clinical Use*; CRC: Boca Raton, FL, 1994.
(2) Bergeron, R. J.; McManis, J. S.; Wiegand, J.; Weimar, W. R. A Search for Clinically Effective Iron Chelators. In *Iron Chelators: New Development Strategies*; Badman, D. G., Bergeron, R. J., Brittenham, G. M., Eds.; Saratoga: Ponte Vedra Beach, FL, 2000; pp 253−292.
(3) Crichton, R. R. *Inorganic Biochemistry of Iron Metabolism*; J. Wiley & Sons: Chichester, U.K., 2001.
(4) Chipperfield, J. R.; Ratledge, C. Salicylate Is Not a Bacterial Siderophore: A Theoretical Study. *BioMetals* **2000**, *13*, 165–168.
(5) Bernier, G.; Girijavallabhan, V.; Murray, A.; Niyaz, N.; Ding, P.; Miller, M. J.; Malouin, F. Desketoneoenactin−Siderophore Conjugates for Candida: Evidence of Iron Transport-Dependent Species Selectivity. *Antimicrob. Agents Chemother.* **2005**, *49*, 241–248.
(6) Walz, A. J.; Mollmann, U.; Miller, M. J. Synthesis and Studies of Catechol-Containing Mycobactin S and T Analogs. *Org. Biomol. Chem.* **2007**, *5*, 1621–1628.
(7) Yuan, W. M.; Gentil, G. D.; Budde, A. D.; Leong, S. A. Characterization of the *Ustilago maydis sid2* Gene, Encoding a Multidomain Peptide Synthetase in the Ferrichrome Biosynthetic Gene Cluster. *J. Bacteriol.* **2001**, *183*, 4040–4051.
(8) Byers, B. R.; Arceneaux, J. E. Microbial Iron Transport: Iron Acquisition by Pathogenic Microorganisms. *Met. Ions Biol. Syst.* **1998**, *35*, 37–66.
(9) Kalinowski, D. S.; Richardson, D. R. The Evolution of Iron Chelators for the Treatment of Iron Overload Disease and Cancer. *Pharmacol. Rev.* **2005**, *57*, 547–583.
(10) Bergeron, R. J. Iron: A Controlling Nutrient in Proliferative Processes. *Trends Biochem. Sci.* **1986**, *11*, 133–136.
(11) Theil, E. C.; Huynh, B. H. Ferritin Mineralization: Ferroxidation and Beyond. *J. Inorg. Biochem.* **1997**, *67*, 30.
(12) Ponka, P.; Beaumont, C.; Richardson, D. R. Function and Regulation of Transferrin and Ferritin. *Semin. Hematol.* **1998**, *35*, 35–54.
(13) Bergeron, R. J.; McManis, J. S. Synthesis of Catecholamide and Hydroxamate Siderophores. In *CRC Handbook of Microbial Iron Chelates*; Winkelmann, G., Ed.; CRC: Boca Raton, FL, 1991; pp 271−307.
(14) Ratledge, C.; Dover, L. G. Iron Metabolism in Pathogenic Bacteria. *Annu. Rev. Microbiol.* **2000**, *54*, 881–941.
(15) Nicholson, M. L.; Beall, B. Disruption of *tonB* in *Bordetella bronchiseptica* and *Bordetella pertussis* Prevents Utilization of Ferric Siderophores, Haemin, and Haemoglobin as Iron Sources. *Microbiology* **1999**, *145*, 2453–2461.
(16) Occhino, D. A.; Wyckoff, E. E.; Henderson, D. P.; Wrona, T. J.; Payne, S. M. *Vibrio cholerae* Iron Transport: Haem Transport Genes Are Linked to One of Two Sets of *tonB*, e*xbB*, *exbD* Genes. *Mol. Microbiol.* **1998**, *29*, 1493–1507.
(17) Stojiljkovic, I.; Srinivasan, N. *Neisseria meningitidis tonB, exbB*, and *exbD* Genes: Ton-Dependent Utilization of Protein-Bound Iron in Neisseriae. *J. Bacteriol.* **1997**, *179*, 805–812.
(18) Griffiths, E.; Williams, P. H. *The Iron-Uptake Systems of Pathogenic Bacteria, Fungi, and Protozoa*, 2nd ed.; John Wiley & Sons: Chichester, U.K., 1999.
(19) Ochsner, U. A.; Johnson, Z.; Vasil, M. L. Genetics and Regulation of Two Distinct Haem-Uptake Systems, *phu* and *has*, in *Pseudomonas aeruginosa*. *Microbiology* **2000**, *146*, 185–198.
(20) Stoebner, J. A.; Payne, S. M. Iron-Regulated Hemolysin Production and Utilization of Heme and Hemoglobin by *Vibrio cholerae*. *Infect. Immun.* **1988**, *56*, 2891–2895.
(21) Drechsel, H.; Winkelmann, G. Iron Chelation and Siderophores. In *Transition Metals in Microbial Metabolism*; G. Winkelmann, C. J. C., Ed.; Harwood Academic: Amsterdam, The Netherlands, 1997; pp 19.
(22) Neilands, J. B. Siderophores: Structure and Function of Microbial Iron Transport Compounds. *J. Biol. Chem.* **1995**, *270*, 26723–26726.
(23) Telford, J. R.; Raymond, K. N. Siderophores. In *Comprehensive Supramolecular Chemistry*; Atwood, J. L., Davies, J. E. D., MacNicol, D. D., Vogtle, F., Lehn, J.-M., Eds.; Elsevier Science: Oxford, U.K., 1996; Vol. 1, pp 245−266.
(24) Winkelmann, G. *CRC Handbook of Microbial Iron Chelates*; CRC: Boca Raton, FL, 1991.
(25) Winkelmann, G.; Drechsel, H. *Microbial Siderophores. Biotechnology*, 2nd ed.; Verlag Chemie: Weinheim, Germany, 1997; Vol. 7.
(26) Bergeron, R. J.; Phanstiel, O., IV. The Total Synthesis of Nannochelin: A Novel Cinnamoyl Hydroxamate-Containing Siderophore. *J. Org. Chem.* **1992**, *57*, 7140–7143.
(27) Bergeron, R. J.; McManis, J. S. Synthesis and Biological Activity of Hydroxamate-Based Iron Chelators. In *The Development of Iron Chelators for Clinical Use*; Bergeron, R. J., Brittenham, G. M., Eds.; CRC: Boca Raton, FL, 1994; pp 237−273.
(28) Bergeron, R. J.; Pegram, J. J. An Efficient Total Synthesis of Desferrioxamine. *J. Org. Chem.* **1988**, *53*, 3131–3134.
(29) Bergeron, R. J.; McManis, J. S. The Total Synthesis of Desferrioxamines E and G. *Tetrahedron* **1990**, *46*, 5881–5888.
(30) Bergeron, R. J.; McManis, J. S. Total Synthesis of Bisucaberin. *Tetrahedron* **1989**, *45*, 4939–4944.
(31) Bergeron, R. J.; McManis, J. S.; Perumal, P. T.; Algee, S. E. The Total Synthesis of Alcaligin. *J. Org. Chem.* **1991**, *56*, 5560–5563.
(32) Bergeron, R. J.; Xin, M. G.; Weimar, W. R.; Smith, R. E.; Wiegand, J. Significance of Asymmetric Sites in Choosing Siderophores as Deferration Agents. *J. Med. Chem.* **2001**, *44*, 2469–2478.
(33) Bergeron, R. J.; Kline, S. J. Short Synthesis of Parabactin. *J. Am. Chem. Soc.* **1982**, *104*, 4489–4492.
(34) Bergeron, R. J.; McManis, J. S.; Dionis, J. B.; Garlich, J. R. An Efficient Total Synthesis of Agrobactin and Its Gallium(III) Chelate. *J. Org. Chem.* **1985**, *50*, 2780–2782.
(35) Bergeron, R. J.; Garlich, J. R.; McManis, J. S. Total Synthesis of Vibriobactin. *Tetrahedron* **1985**, *41*, 507–510.
(36) Bergeron, R. J.; Bharti, N.; Singh, S. Total Synthesis of Vulnibactin: A Natural Product Iron Chelator. *Synthesis* **2007**, *7*, 1033–1037.
(37) Kim, C.-M.; Park, Y.-J.; Shin, S.-H. A Widespread Deferoxamine-Mediated Iron-Uptake System in *Vibrio vulnificus*. *J. Infect. Dis.* **2007**, *196*, 1537–1545.
(38) Stoebner, J. A.; Butterton, J. R.; Calderwood, S. B.; Payne, S. M. Identification of the Vibriobactin Receptor of *Vibrio cholerae*. *J. Bacteriol.* **1992**, *174*, 3270–3274.
(39) Butterton, J. R.; Stoebner, J. A.; Payne, S. M.; Calderwood, S. B. Cloning, Sequencing, and Transcriptional Regulation of *viuA*, the Gene Encoding the Ferric Vibriobactin Receptor of *Vibrio cholerae*. *J. Bacteriol.* **1992**, *174*, 3729–3738.
(40) Simpson, L. M.; Oliver, J. D. Siderophore Production by *Vibrio vulnificus*. *Infect. Immun.* **1983**, *41*, 644–649.
(41) Okujo, N.; Akiyama, T.; Miyoshi, S.; Shinoda, S.; Yamamoto, S. Involvement of Vulnibactin and Exocellular Protease in Utilization of Transferrin- and Lactoferrin-Bound Iron by *Vibrio vulnificus*. *Microbiol. Immunol.* **1996**, *40*, 595–598.
(42) Webster, A. C. D.; Litwin, C. M. Cloning and Characterization of *vuuA*, a Gene Encoding the *Vibrio vulnificus* Ferric Vulnibactin Receptor. *Infect. Immun.* **2000**, *68*, 526–534.
(43) Henderson, D. P.; Payne, S. M. *Vibriobactin cholerae* Iron Transport Systems: Roles of Heme and Siderophore Iron Transport in Virulence and Identification of a Gene Associated with Multiple Iron Transport Systems. *Infect. Immun.* **1994**, *62*, 5120–5125.
(44) Litwin, C. M.; Rayback, T. W.; Skinner, J. Role of Catechol Siderophore Synthesis in *Vibrio vulnificus* Virulence. *Infect. Immun.* **1996**, *64*, 2834–2838.
(45) Stelma, G. N.; Reyes, A. L.; Peeler, J. T.; Johnson, C. H.; Spaulding, P. L. Virulence Characteristics of Clinical and Environmental Isolates of *Vibrio vulnificus*. *Appl. Environ. Microbiol.* **1992**, *58*, 2776–2782.
(46) Miller, M. J.; Malouin, F. Siderophore-Mediated Drug Delivery: The Design, Synthesis, and Study of Siderophore-Antibiotic and Antifungal

Conjugates. In *The Development of Iron Chelators for Clinical Use*; Bergeron, R. J., Brittenham, G. M., Eds.; CRC: Boca Raton, FL, 1994; pp 275−306.
(47) Esteve-Gassent, M. D.; Amaro, C. Immunogenic Antigens of the Eel Pathogen *Vibrio vulnificus* Serovar E. *Fish Shellfish Immunol.* **2004**, *17*, 277–291.
(48) Griffiths, G. L.; Sigel, S. P.; Payne, S. M.; Neilands, J. B. Vibriobactin, a Siderophore from *Vibrio cholerae*. *J. Biol. Chem.* **1984**, *259*, 383–385.
(49) Payne, S. M.; Finkelstein, R. A. Siderophore Production by *Vibrio cholerae*. *Infect. Immun.* **1978**, *20*, 310–311.
(50) Crosa, J. H. Signal Transduction and Transcriptional and Posttranscriptional Control of Iron-Regulated Genes in Bacteria. *Microbiol. Mol. Biol. Rev.* **1997**, *61*, 319–336.
(51) Crosa, J. H. Molecular Genetics of Iron Transport as a Component of Bacterial Virulence. In *Iron and Infection: Molecular, Physiological, and Clinical Aspects*, 2nd ed.; Bullen, J. J., Griffiths, E., Eds.; John Wiley & Sons: Chichester, U.K., 1999; pp 255−288.
(52) Litwin, C. M.; Calderwood, S. B. Role of Iron in Regulation of Virulence Genes. *Clin. Microbiol. Rev.* **1993**, *6*, 137–149.
(53) Bergeron, R. J.; Weimar, W. R.; Müller, R.; Zimmerman, C. O.; McCosar, B. H.; Yao, H.; Smith, R. E. Synthesis of Reagents for the Construction of Hypusine and Deoxyhypusine Peptides and Their Application as Peptidic Antigens. *J. Med. Chem.* **1998**, *41*, 3888–3900.
(54) Oshima, T. Unique Polyamines Produced by an Extreme Thermophile, *Thermus thermophilus*. *Amino Acids* **2007**, *33*, 367–372.
(55) Bergeron, R. J.; Bharti, N.; Wiegand, J.; McManis, J. S.; Yao, H.; Prokai, L. Polyamine-Vectored Iron Chelators: The Role of Charge. *J. Med. Chem.* **2005**, *48*, 4120–4137.
(56) Bergeron, R. J.; Kline, S. J. 300 MHz ^{1}H NMR Study of Parabactin and Its Gallium(III) Chelate. *J. Am. Chem. Soc.* **1984**, *106*, 3089–3098.
(57) Fletcher, S.; Gunning, P. T. Mild, Efficient and Rapid O-Debenzylation of Ortho-Substituted Phenols with Trifluoroacetic Acid. *Tetrahedron Lett.* **2008**, *49*, 4817–4819.
(58) *Coomassie Plus—The Better Bradford Assay Kit*; Pierce: Rockford, IL 23236.
(59) Bergeron, R. J.; Weimar, W. R. Kinetics of Iron Acquisition from Ferric Siderophores by *Paracoccus denitrificans*. *J. Bacteriol.* **1990**, *172*, 2650–2657.
(60) Kao, K.-J.; Klein, P. A. A Monoclonal Antibody-Based Enzyme-Linked Immunosorbent Assay for Quantitation of Plasma Thrombospondin. *Am. J. Clin. Pathol.* **1986**, *86*, 317–323.
(61) Simrell, C. R.; Klein, P. A. Antibody Responses of Tumor-Bearing Mice to Their Own Tumors Captured and Perpetuated as Hybridomas. *J. Immunol.* **1979**, *123*, 2386–2394.
(62) Bergeron, R. J.; Streiff, R. R.; Creary, E. A.; Daniels, R. D., Jr.; King, W.; Luchetta, G.; Wiegand, J.; Moerker, T.; Peter, H. H. A Comparative Study of the Iron-Clearing Properties of Desferrithiocin Analogues with Desferrioxamine B in a *Cebus* Monkey Model. *Blood* **1993**, *81*, 2166–2173.
(63) Bergeron, R. J.; Streiff, R. R.; Wiegand, J.; Vinson, J. R. T.; Luchetta, G.; Evans, K. M.; Peter, H.; Jenny, H.-B. A Comparative Evaluation of Iron Clearance Models. *Ann. N.Y. Acad. Sci.* **1990**, *612*, 378–393.
(64) Thermo Fisher Scientific. Extinction Coefficients. http://www.piercenet.com/files/TR0006dh5-Extinction-coefficients.pdf.
(65) Bergeron, R. J.; Wiegand, J.; McManis, J. S.; McCosar, B. H.; Weimar, W. R.; Brittenham, G. M.; Smith, R. E. Effects of C-4 Stereochemistry and C-4′ Hydroxylation on the Iron Clearing Efficiency and Toxicity of Desferrithiocin Analogues. *J. Med. Chem.* **1999**, *42*, 2432–2440.
(66) Imject Maleimide Activated BSA and OVA Kits Instructions; Pierce: Rockford, IL; Product Nos. 77112, 77113.

JM900119Q